Role for serotonergic neurons of the parapyramidal region in the control of locomotion revealed using chemogenetic activation in Tph2-cre driver rats

by

Katrina Armstrong

A Thesis submitted to the Faculty of Graduate Studies of

The University of Manitoba

in partial fulfilment of the requirements of the degree of

MASTER OF SCIENCE

Department of Physiology and Pathophysiology

University of Manitoba

Winnipeg

Abstract

Several brainstem regions are necessary to provide transmission of a descending signal to motor networks within the lower the limbs. The Parapyramidal region (PPR) within the ventrolateral medulla appears to play an important but yet unspecified role in locomotion. The recent advent of DREADDs (Designer Receptors Exclusively Activated by Designer Drugs) has allowed for non-invasive in vivo manipulation of neurons. DREADDs were stereotaxically injected into the PPR using adeno-associated viral vectors (AAVs). After a recovery period, rats were tested in both voluntary (open field) and fictive locomotion experiments to evaluate motor activity after administration of the DREADD actuator. Immunohistochemical detection confirmed DREADDs within the PPR. Locomotor activity increased significantly (172%) after DREADD activation during open field locomotor testing. With electrical stimulation, burst duration was significantly increased (174%) in flexor hindlimb nerves. Chemogenetic activation of the PPR seems to facilitate hindlimb motor output but specific effects on fictive locomotion were inconclusive.

Acknowledgements

I would like to thank my committee members **Dr. Brent Fedirchuk** and **Dr. Sari Hannila** for all of their valuable input during my Master's program. In addition, if it was not for **Brent** and **Matt Ellis**, I would have never been introduced to the Wednesday morning hockey group and the Kahula cup. I am still dreaming of the day when I can hold the cup up high for Team Black.

I would like to thank my supervisors, **Dr. Larry Jordan** and **Dr. Katinka Stecina**, for their patience and mentorship. It is inspiring to be around people who truly enjoy learning. Words can't express how grateful I am to the opportunities they have given me. It has been wonderful to receive encouragement during my research project as well as the friendship that has developed along the way. I am extremely excited for what we will achieve in the near future.

Thank you to my fellow graduate colleagues at the SCRC; **Sarah (Xiaoyu)** for her infectious laugh and stories, **Ramiro** for the many coffee breaks, and to **Mona,** for all of the support during the frustrating times as well as the lengthy discussions about science and life. Furthermore, I would like to thank the technicians within the lab, **Erika** and **Xicheng,** who were the quiet heroes behind the scene. Thank you to **Gail**, **Judy**, **Gilles**, **Maria**, and **Sharon** for all their technical and administrative assistance. Thank you for to the rest of the members of the **SCRC** (as well as **Maria** the caretaker) who would greet me with a smile. These people truly embody "Friendly Manitoba".

I would like to thank the community of Winnipeg for welcoming me with opening arms. Thank you to **St. Boniface Golf Club** and **Niakwa Country Club** and the members for the remarkable golfing experience. Thank you to **Winnipeg Ball Hockey Association**, **Manitoba Ball Hockey,** and **Winnipeg Winter Club** and the members of these associations**.** I have developed lifelong friendships and played some fantastic hockey along the way.

I have to especially thank the **Smaczylo/Goodman** families for accepting me as a daughter in Winnipeg. **Sylvia, Brian, Brittany, Alex, Horace, Mandy, Sabrina, Dustin,** and friends of the family. Thank you for giving me a place where I could be myself and being my home away from home.

Thank you to my family; **Stephanie**, **Derek**, **Mitchell**, **Gary**, **Susan**, **Jacqui**, **Chelsey**, **Jordan**, **Adam**, **Jodi**, **Rylan**, **Tyler**, **Jake** and **Tiger Lily**. Special thanks to my Aunt **Lesia Proverbs** for her editing suggestions. I am so lucky to have the support of my family.

As Arnold Schwarzenegger says, "I am not a self-made man. I got a lot of help." Thank you to all the parents, coaches, teachers, mentors, and friends who have given me advice and assistance along the way.

Dedication

In loving memory of my father, Ronald Armstrong, who instilled the values of perseverance and curiosity.

Most importantly to my mother, Stephanie Graham, for her constant unconditional love and support.

Table of Contents

List of Tables

List of Figures

List of Common Acronyms

5-HT	5-hydroxytryptamine
C21	Compound 21
CnF	Cuneiform Nucleus
CNO	Clozapine-n-oxide
CP	Common peroneal
CPG	Central pattern generator
DIO	Double inverted open reading frame
DREADD	Designer receptor exclusively activated by designer drug
ENG	Electroneurogram
fMRI	Functional magnetic resonance imaging
hM3Dq	Gq-coupled human M3 muscarinic DREADD
iCre	Codon-optimized cre
LPGi	Lateral paragigantocellular nucleus
MLR	Mesencephalic locomotor region
PET	Positron-emission tomography
PMRF	Pontomedullary reticular formation
PPN	Pedunculopontine nucleus
PPR	Parapyramidal region
rAAV	Recombinant Adeno-associated virus
RS	Reticulospinal
Tib	Tibial
Tph2	Tryptophan hydroxylase 2
VLF	Ventrolateral funiculus

Chapter 1. Introduction

1.1. The Mesencephalic Locomotor Region (MLR)

Although higher brain centres are necessary for the fine control of locomotion, the initiation of locomotion can be deconstructed into a relatively simple hierarchy. Neural signals from higher brain regions activate brainstem locomotion initiating centers, which then in turn activate spinal networks leading to coordinated movements of the muscles and limbs. The mesencephalon, in particular, is accepted as an important site for the initiation of locomotion. Shik and colleagues (1966) demonstrated that electrically stimulating (either unilateral or bilateral) a definite midbrain region, the mesencephalic locomotor region (MLR), was sufficient to elicit well-coordinated activity within the lower limbs (Shik et al. 1966). By increasing the intensity of stimulation, the elicited response could reliably transition from walk to trot to gallop (Shik et al. 1966). This fine control of locomotion is one of the most remarkable features of the MLR. Although it is still debated which nuclei constitute the MLR (Ryczko and Dubuc 2013), ample evidence suggests that the cuneiform (CnF) and subcuneiform regions are more effective (Ryczko and Dubuc 2013) rather than the pedunculopontine nuclei (PPN) (Takakusaki et al. 2016; Noga et al. 2017; Roseberry et al. 2016). Stimulating the MLR to produce movement seems to be conserved across the vertebrate phylum (For review see Ryczko and Dubuc 2013) and stimulation of the MLR in a decerebrate rat also evokes locomotion (Skinner and Garcia-Rill 1984). In recent years, advances in technology have made it possible to dissect the function of identified neuronal populations, such as the MLR. Using optogenetic constructs within the MLR, Lee and colleagues were able to reliably generate locomotion using optogenetic activation of this region (Lee et al. 2014). Within this approach, the viral construct they used preferentially

targeted glutamatergic neurons, but it is known that the MLR is a heterogeneous structure, with several subpopulations of neurons (Thankachan et al. 2012). In this case, future studies should focus on dissecting the specific contributions of multiple cell types that send descending projections to locomotor regions (Lee et al. 2014). The combination of mouse genetics and viral tools available allows these types of investigations to be feasible at this time.

1.2. The Reticulospinal System (RS)

The descending fibres from the MLR in the cat do not project directly to the spinal cord, but rather synapse bilaterally with reticulospinal (RS) neurons in the pontomedullary reticular formation (PMRF) (Shik and Orlovsky 1976). As outlined in figure 1.1., these RS neurons have axons that travel to the spinal cord via the ventral lateral funiculus (VLF) (Jordan 1986) and appear to be the major relay from higher brain motor command centres to the spinal cord (Drew et al. 1986). As indicated above, increasing MLR stimulation can progressively increase the speed of locomotor movements, which also leads to a growing activation of RS cells (Ryczko et al. 2017). Accordingly, cooling the PMRF to prevent synaptic transmission (Noga et al. 2003) produces major locomotor deficits. The descending RS neurons are known to have extensive axonal branching and can form various contacts, excitatory or inhibitory, with limb motoneurons (Riddle et al. 2009; Peterson 1979). Thankachan and colleagues (2012) were able to associate neural firing of non-cholinergic RS neurons with motor behaviors, which indicates that these cells may be regulating the motor commands from the MLR (Thankachan et al. 2012). The collective evidence suggests that the RS cells are the mediators of MLR-evoked fictive locomotion and have direct access to spinal central pattern generators (CPGs) (Armstrong 1986), as shown in figure 1.1.

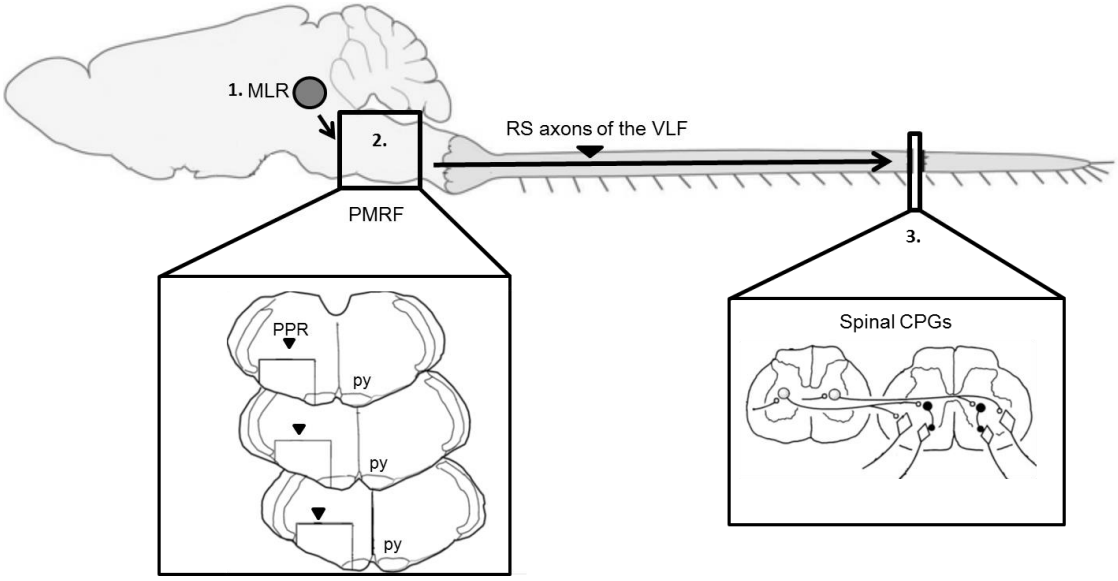

Figure 1.1. Descending pathway from parapyramidal region activating spinal central pattern generators.

The parapyramidal region (PPR) (2) is located bilaterally within the ventral medulla next to the pyramidal tracts (py) within the region known as the pontomedullary reticular formation (PMRF). Neurons in the mesencephalic locomotor region (MLR) (1) transmit a locomotor command signal to this region (2) and activate reticulospinal (RS) neurons. These RS neurons contain a group of serotonergic neurons that project down the spinal cord mainly via the ventrolateral funiculus (VLF) and make contacts on interneurons within the central pattern generator (CPG) (3). The CPG can produce basic rhythmic and coordinated locomotor movements.

1.3. Central Pattern Generators involved in locomotion

While the above summary outlines the descending control of locomotion arising from the brainstem, neural circuits located within the spinal cord are responsible for integrating this information and fine-tuning the locomotor output signals to the muscles. These spinal neural circuits, however, are able to self-produce rhythmic activity even in the absence of supraspinal or sensory-derived signals (Grillner and El Manira 2015). Graham Brown was the first to describe this pattern-generating circuitry, wherein he demonstrated alternating activity in antagonist muscles after transection of the spinal cord (Reviewed by Stuart and Hultborn 2008). The central hypothesis is that there are networks of spinal neurons, known as CPGs that serve to produce the

basic motor program (Reviewed by Grillner and El Manira 2015; Kiehn 2016; McCrea and Rybak 2008)

There has been debate about the degree to which the locomotor CPG is localized to specific thoracolumbar spinal segments versus distributed across a wide range of segments. While it is clear that CPG elements are apparent in upper lumbar (e.g. L1 and L2) segments (Grillner and Zangger 1979), the CPG has clearly been demonstrated to be distributed across a variety of other spinal segment levels, specifically within the thoracolumbar spinal cord (Cazalets et al. 1995; Cowley and Schmidt 1997; Kjaerulff and Kiehn 1996). As described above, CPGs can be activated by several pathways, including inputs from the RS cells of the brainstem.

There are several neurotransmitters and modulators known to be involved in locomotion, mostly identified from research using the isolated spinal cord preparation of neonatal rodents. In these preparations it has been shown that several agonists of N-methyl-d-aspartate (NMDA), noradrenaline (NA), 5-hydroxytryptamine (5-HT), dopamine (DA), and acetylcholine (ACh) can generate rhythmic activity resembling locomotion (see review by Jordan et al. 2008). In addition, many of these neurotransmitters, except cholinergic, have been found to descend from the RS cells of the PMRF (Jordan et al. 2008). In particular, the 5-HT neurons are known to have spinally-projecting neurons implicated in the initiation of locomotion (Jordan et al. 2008).

1.4. Location of descending serotonergic projections

Serotonin, also known as 5-HT, is a monoamine neurotransmitter that is present in both the CNS and within the gastrointestinal tract (Tyce 1990). Within the mammalian spinal cord, all 5-HT-positive axons originate from the raphe nuclei of the brainstem and adjoining ventral

reticular formation (Dahlström and Fuxe 1964). Dahlstrom and Fuxe (1964) were the first to describe the distribution of 5-HT in the rat brainstem and classified nine subpopulations (B1-B9) of 5-HT containing cells (Dahlström and Fuxe 1964). The descending projections arise from the midline B1 (raphe pallidus) and B2 (raphe obscurus) areas, as well as lateral to the B3 (raphe magnus) area (Dahlström and Fuxe 1964). In rats, these nuclei are known to innervate all laminae within the spinal cord (Bowker et al. 1981; Skagerberg and Björklund 1985) and nearly all of the 5-HT in the lumbar spinal cord in mammals originates from these areas (reviewed by Schmidt and Jordan 2000). The 5-HT fibers of the B1 and B2 areas terminate in the ventral horn (Rajaofetra et al. 1989; Skagerberg and Björklund 1985) and 99% of these axons are co-localized with substance P (Schmidt and Jordan 2000). 5-HT can also innervate the dorsal horn but the highest density is found in the ventral horn (Steinbusch 1981).

1.5. Functions of descending 5-HT

The descending 5-HT system has a large number of functions, contributing to the motor system, neuroendocrine functions, sensory processing, and autonomic outflows. These neurons most likely act synergistically to coordinate the interaction between these systems. As Kerman and colleagues stated “CNS neurons that innervate both sympathetic and motor outflows; it seems likely that these neurons play a role in concomitant regulation of sympathetic and motor efferent activities during behaviours that require such coordination, such as exercise" (Kerman et al. 2003). During locomotion and other forms of exercise, the body needs to coordinate motor output with immediate increases in other autonomic systems such as respiration and cardiovascular function (Waldrop et al. 2011). For example, the 5-HT neurons that innervate face and neck muscles must coordinate respiration and muscle activities simultaneously to prevent aspiration of oral contents during chewing (Hennessy et al. 2017). The hypothesized functions of

the descending 5-HT system is to facilitate motor output, while simultaneously suppressing sensory information and processing (Jacobs and Fornal 1993).

Although 5-HT plays an important role in anti-nociception, autonomic function, breathing, sexual function, and sleep-wake cycles, the focus of further discussion will be on the role of 5-HT in modifying locomotion. This is an important topic as neuronal injuries affecting communication between brain and spinal cells often involves the loss of descending serotonergic input to spinal targets. Recovery of motor function after spinal cord injury (SCI), for example, has been shown to greatly correlate with the degree of innervation of lumbar motoneurons.

1.6. *In vitro* evidence that 5-HT facilitates locomotor networks

While the *in vivo* decerebrate cat preparation has been important in determining the initiation of locomotion as well as the effects of sensory feedback in motor patterning (Whelan 1996), the use of the *in vitro* neonatal spinal cord preparation (Kudo and Yamada 1987) has been invaluable to determine the neurochemical substrates of mammalian locomotion (Smith and Feldman 1987). Several studies have shown that bath application with a variety of neurotransmitters may elicit locomotor-like behaviour or activate the locomotor network in the isolated spinal cord preparation. However, in both neonatal mice and rats, the most effective neurotransmitter to elicit activity seems to be 5-HT (Schmidt and Jordan 2000). Moreover, 5-HT seems to produce a more stable and faster locomotor rhythm (Kjaerulff and Kiehn 1996). The most effective site to elicit this activity was limited to the supralumbar segments of the cord (Cowley and Schmidt 1997) consistent with the notion that all sources of the 5-HT released are in the brainstem.

1.7. *In vivo* evidence that 5-HT facilitates locomotor networks

Several studies suggest that 5-HT may elicit and modulate locomotor behaviour. First and foremost, it is released during motor activity (Gerin and Privat 1998), and the source neurons exhibit increased firing rates in response to a locomotor task (Veasey et al. 1995; Jacobs et al. 2002). Descending 5-HT is presumed to activate the CPG (Cazalets et al. 1992), and a strategy to help regain some locomotor function has been to partially reinstitute the missing neurotransmitters below a spinal cord lesion. Using grafts of embryonic 5-HT cells, Gimenez y Ribotto et al (2000) showed that spinalized rats were able to regain a full pattern of hind limb locomotion after cell transplant *in vivo* (Ribotta et al. 2000). Although these T11 transplants were successful, the T9 animals showed no functional recovery, suggesting that innervating by 5-HT within the L1-L2 level is essential for the generating rhythmic locomotor activity (Ribotta et al. 2000). Further research from Slawinska and colleagues (2013) showed that grafting neurons destined to form the B1, B2 and B3 regions effectively restores coordinated plantar stepping. Much of the data suggests that 5-HT_2 and 5-HT_7 are necessary for recovering locomotor capability and activation of both receptor subtypes is a more effective strategy after SCI (Sławińska et al. 2013).

1.8. The 5-HT receptor subtypes and their differential contribution to locomotor function

The 5-HT system consists of seven families of receptors (5-HT 1-7) with at least 14 distinct receptor subtypes. These receptor subtypes are distributed through the laminae within the spinal cord. 5-HT receptors are primarily G-protein coupled metabotropic receptors, while the 5-HT_3 receptor family is a ligand gated ion channel (Barnes and Sharp 1999).

Initially, it was thought that activation of multiple 5-HT receptor subtypes contributed during locomotion (Cazalets et al. 1992) but this notion has changed with the development of more specific agonists and antagonists (Madriaga et al. 2004). Several lines of evidence suggest that 5-HT_7, 5-HT_{2A} and 5-HT_{1A} appear to be the major receptors involved in the production of locomotion (Hochman et al. 2001). Using c-fos, Noga and colleagues show that most locomotor activated cells co-localize with 5-HT_7, 5-HT_{2A} and 5-HT_{1A} receptors (Noga et al. 2009).

Evidence from the Jordan lab obtained from neonatal rats supports the hypothesis that 5-HT_7 receptors may play a critical role in rhythmogenesis of the spinal CPG for locomotion. In this paradigm, elicited locomotor activity from the parapyramidal region (PPR) was completely blocked using the 5-HT_7 antagonist, SB269970 (Liu and Jordan 2005). These PPR 5-HT neurons whose actions appear to be mediated by the 5-HT_7 receptor activation in the spinal cord may constitute a subtype of 5-HT locomotor neurons.

1.9. Serotonergic PPR neurons are important for locomotion by activating spinal 5-HT_7 receptors

A population of 5-HT neurons located next to the pyramidal tracts, the PPR, as mentioned above seems to be important for locomotion (Helke et al. 1989; Jones and Light 1992). This area is synonymous with the lateral paragigantocellular reticular nucleus (LPGi) (Lakke 1997), and it contains the second largest population of 5-HT neurons in the medulla. Previous research in brainstem evoked locomotion has implicated the PPR as an effective means of inducing locomotion (Liu and Jordan 2005) and facilitating locomotion induced by stimulation of the MLR. In decerebrate cats, the 5-HT neurons of the PPR exhibit activity-dependent *Fos* labeling following MLR evoked locomotion (Noga and Opris 2017). Although

the PPR contains a heterogeneous population of neurons, the PPR has been suggested as the source of 5-HT RS neurons that relay a descending locomotor command from the MLR. Furthermore, the 5-HT_7 receptors appear to be the mediators of this serotonergic locomotor pathway. Using SB269970, a 5-HT_7 receptor antagonist, is able to disrupt fictive locomotion in neonatal rodents and voluntary locomotion adult rodents (Liu et al. 2009; Liu and Jordan 2005). However, adult mice lacking 5-HT_7 receptors do not appear to show major deficiencies in locomotion. This is most likely due to the redundancy of descending locomotor systems, and the potential compensation by other descending pathways in the response to the lack of 5-HT.

The effects of PPR neurons on locomotion are much less clear in the adult versus in the neonates. In both adult mice and rats, blockade of 5-HT_7 receptors during voluntary locomotion produces hind limb locomotor impairment (Liu et al. 2009; Cabaj et al. 2017). However, during MLR-evoked fictive locomotion (i.e. in the absence of sensory feedback), coordination does not seem to be altered (Cabaj et al. 2017). These results indicate that 5-HT_7 receptors play an important role in afferent feedback within the adult rat during locomotion, but further research is necessary to determine the role of these receptors.

1.10. The PPR is a major lower brainstem center controlling many physiological processes.

"The cells of the PPR have been variably referred in the literature as the nucleus interfascicularis hypoglossi, nucleus paragigantocellularis pars alpha, medial aspect of the nucleus paragigantocellularis lateralis, parapyramidal nucles, paraolivary nucleus, arcuate nucleus, and the lateral portions of B1 and B3" (Helke, Thor, and Sasek 1989). However, within

the literature, the variability in this terminology that describes this region greatly contributes to the lack of definitions when it comes to its involvement in different physiological functions.

The PPR is presumed to contain multiple transmitter systems, with many of the neurons containing 5-HT and thus it has been considered as a lateral extension of B1 (and B3) neurons (Skagerberg and Björklund 1985). In addition, lateral to the 5-HT containing cells of the PPR, there appears to be a group of nonserotonergic cells that contain vesicular glutamate transporter 2(VGLUT2) mRNA and are thus probably glutamatergic (Weston, Stornetta, and Guyenet 2004). These neurons lack spinal projections, and mostly innervate the dorsolateral pons and ipsilateral ventral respiratory column. They are unlike the serotonergic neurons which heavily innervate the spinal cord (Weston, Stornetta, and Guyenet 2004). The PPR is also immunoreactive for multiple neuropeptides such as substance P (SP), thyrotropin-releasing hormone (TRH), encephalin (ENK), cholecystokinin (CCK), somatostatin, galanin, proctolin, β-lipotropin, and human growth hormone (Helke, Thor, and Sasek 1989).

The neurons within the PPR are likely to function as a lower brainstem center that is involved in cardiovascular control, respiration, thermoregulation, sexual function and pain (Mason 2001). The projections within the intermediolateral cell column (IML) are thought to be important for cardio-regulation (Helke, Thor, and Sasek 1989). In addition, this region is known to send serotonin-containing projections to the rostral ventral respiratory group, suggesting that these neurons may influence respiratory control (Holtman, Marion, and Speck 1990). After pseudorabies virus injection into the penis of rats and retrograde tracing, more than half of the virus-labeled cells were located in the PPR and were mostly serotonergic, providing evidence that this region may contribute to sexual climax motor patterns (Marson, Platt, and McKenna 1993). Further evidence supports that the PPR may contribute to gastric acid secretions. Data

from Yang et al. (1999) show that chemical activation of the PPR with kainate results in a vagal-dependent stimulation of gastric acid secretion. Furthermore, Fos-labelled cells were found in the PPR after exposure to cold, which is known to induce a vagally mediated gastric secretion response (Yang et al. 1999). Taken together the above described evidence suggests that the PPR is a major brainstem center for motor and autonomic regulation. This is by no means an exhaustive list but it serves as an indication of the multitude of homeostatic functions that the PPR is likely to integrate. The research presented in this thesis, however, is focused on the serotonergic neurons with respect to their contribution to hindlimb motor control, specifically to locomotion.

1.11. Statement of problem

The previous studies of serotonergic effects during fictive locomotion were carried out using isolated neonatal rodent spinal cord preparations (Liu and Jordan 2005) but there is evidence that 5-HT has differential functions in neonatal and older rodents (Abbinanti et al. 2012; Husch et al. 2015). There is preliminary data from our lab confirming facilitation of MLR evoked locomotor activity, in vivo in adult rats by electrical stimulation of the PPR when stimulation is applied in a non-specific manner near the ventral surface of the medulla where PPR neurons are located. Nonetheless, standard electrophysiology methods have made it difficult to ascribe the effect to a defined cell population. In other words, previous studies have established a causal relationship between the activation of 5-HT neurons in or near the PPR and locomotion, but lack of specificity has limited the ability to make further conclusions. It still remains to be determined how PPR neurons communicate with locomotor neurons in the spinal cord and whether they are apt to initiate or only facilitate locomotion in adult animals in vivo.

Therefore, the main **hypothesis** to be examined in this study is that stimulation of the PPR in adult rats is sufficient for evoke locomotor activity, and activation of PPR neurons facilitates locomotion.

1.12. Selective stimulation of neural populations by chemogenetic means

G-protein coupled receptors (GPCRs) are metabotropic receptors that mediate many cell signal pathways. GPCRs are responsible for a large variety of physiological processes, from chemosensory recognition to complex behavioural events (Pierce et al. 2002). For numerous biologically active molecules, GPCRs mediate the signal transduction within the cell. Consequently, within the pharmaceutical industry, GPCRs or their downstream targets are of key interest because of their role in regulating a wide variety of human physiological processes. The major challenge has been to create selective ligands that do not bind off target. Ultimately, the ideal pharmaceutical would be able to specifically activate a single G-protein cascade. Recently, researchers have developed a technology in rodents and non-human primates that introduces molecular control switches within the brain. Designer Receptors Exclusively Activated by Designer Drugs (DREADDs) are engineered GPCRs that allow for spatial and temporal control of signalling in vivo by using its synthetic ligand, Clozapine-N-Oxide (CNO) (Urban and Roth 2015). The Gq-DREADD (hM3Dq) permits specific Gq-mediated signalling leading to neuron depolarization and potentially cell firing (Alexander et al. 2009). The posited benefits of hM3Dq includes a platform that replicates native M3 muscarinic receptor activation by acetylcholine but with no apparent constitutive activity (Urban and Roth 2015). CNO is advertised as being pharmacologically inert, orally bioavailable, CNS penetrant and not subject to significant metabolic transformation in rodents (Chen et al. 2015). hM3dq activation in neurons may enhance neural excitability which can lead to burst like firing (Alexander et al. 2009).

In order to deliver the sequence of chemogenetic receptors into neurons or other cell types, researchers can use genetic models that inherently contain these DREADDs, or deliver these constructs using replication defective viral vectors (e.g. lentivirus, LV or adeno-associated viral vectors, AAV) (Urban and Roth 2015). While using viral delivery methods, AAVs are preferred as they are safer and do not integrate within the host DNA which reduces the potential for normal transcription being disrupted (Samulski and Muzyczka 2014). In order to ensure targeted expression of chemogenetic constructs, it is necessary to use localized injections. Normally, viral vector solutions injected have limited diffusion capabilities, as only cells within a few millimeters of the site are transduced (Davidson and Breakefield 2003). To overcome this problem of limited diffusion, larger injection volumes and/or using multiple injection tracks have been the best strategies to transfect more cells (Davidson and Breakefield 2003). In order to get neuron specific expression of DREADDs, a cre recombinase mediated strategy is used. By using Cre-dependent AAVs, DREADD expression can be restricted to cells that selectively express Cre (Whissell et al. 2016). In combination with stereotaxic microinjections, Cre-dependent AAVs allow for selective targeting of DREADDs to a subpopulation of neurons that may contain several different cell types (see Figure 1.2).

1.13. Chemogenetic control of serotonergic neural signaling

While 5-HT was described in relation to its descending functions, it also has extensive efferent projections to the forebrain. Metabotropic 5-HT receptors within these areas are directly or indirectly associated with several psychiatric medications as well as the sites of action for many drugs of abuse (Charnay and Léger 2010). The elicited physiological effect is dependent upon the area and cellular distribution of different 5-HT receptor subtypes. Until now, our understanding of both ascending and descending raphe subgroups has been based upon

pharmacological application and lesion studies. Both methods lack specificity, as pharmacological methods may have off-target effects and lesion studies cause permanent and irreversible damage. By using DREADDs, researchers are now able to target neuron populations specifically and reversibly. For example, the Dymecki laboratory has generated mouse models for transcriptional profiling of individual 5-HT neurons for functional studies in order to determine the role of these subtypes in respiration. Ray et al. (2011) pioneered the first study of hM4Di perturbation of *Slc6a4-cre* expressing neurons to examine the respiratory chemoreflex in a CO_2 chamber. After CNO administration, the normal increase in respiration response was altered by 50% as well as a drastic response in body temperature (from 36.9ºC to 27.1ºC) (Ray et al. 2011). Further investigations by Ray et al. (2013) targeted a more specific population of 5-HT neurons (the early growth response 2 transcription factor, *Egr2*) essential for breathing in neonates but never examined in adults. Perturbing these neurons blunted the ventilatory response but did not alter thermoregulation (Ray et al. 2013). To determine which serotonergic subgroups were truly chemosensitive, Brust et al. (2014) manipulated the developmentally defined serotonergic subgroups one-by-one. R5Egr2-Pet1 neurons were found to be intrinsically chemosensitive, increasing firing in response to hypercapnic acidosis, collectively indicating a role as chemoreceptors that facilitate respiratory drive (Brust et al. 2014). These neurons, however, do not make contacts on respiratory motoneurons. Hennessy et al. (2017) suspected that double-positive 5-HT/substance P neurons i.e. *Tac1-Pet1* neurons may innervate the respiratory motor nuclei and confirmed this hypothesis. r5Egr2-Pet1 neurons subtype is involved in detection and processing of CO_2 chemosensory input signals (Brust et al. 2014). The Tac1-Pet1 subtype are likely involved in the modulation of respiratory motor output and rhythm generation (Hennessy et al. 2017).

Resolution of 5-HT neuron specific functions helps to reconcile debates regarding 5-HT neurons and function. For example, some authors argued against a 5-HT neuron chemoreceptive function (Depuy et al. 2011), but further research using DREADDs has supported the role of these neurons in chemoreception (Hennessy et al. 2017).

The descending 5-HT in the CNS can make multiple contacts on different metabotropic receptor subtypes with opposing actions on signal transduction pathways. Consequently, there may be regional differences in 5-HT function depending on the descending subgroup that is activated. It is apparent that there is a gap in the literature, as there are very few studies using chemogenetics to elucidate the functions 5-HT descending pathways. Moreover, previous research has not utilized chemogenetics to determine the role of 5-HT in locomotion.

1.14. Objectives of this study

Objective 1. Demonstrate that electrical stimulation limited to the vicinity of the PPR in the adult rat facilitates midbrain-stimulation evoked locomotor activity.

Uses of knockout models without serotonergic neurons does not produce overt changes in locomotion and this can be attributed to the considerable redundancy in descending command pathways for the initiation of locomotion. The *Tph2* rat model can be used for *Cre*-dependent transfection of PPR neurons by DREADDs.

Objective 2. Demonstrate that selective activation of PPR neurons by chemogenetic means utilizing the DREADD technology can initiate locomotion and/or facilitate midbrain-evoked fictive locomotor activity.

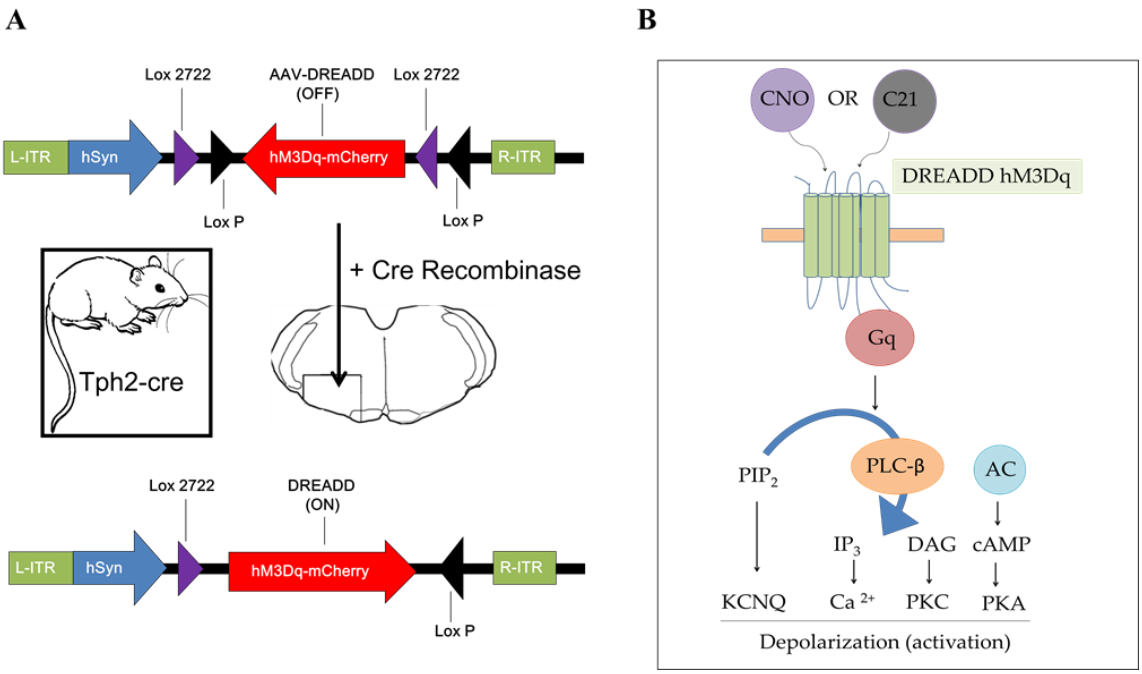

Figure 1.2 Expression and activation of DREADDs in Tph2-iCre Rats

A. Experimental design: unilateral or bilateral injections of the rAAV-hSyn-DIO-hM3Dq-mCherry are placed into the PPR of *Tph2-Cre* rats. After a cre-mediated recombination event, hM3Dq is inverted to sense resulting in expression of hM3Dq in 5-HT PPR neurons. The dissimilar lox sites (loxP and lox 2272) confers a permanent recombination event.

B. A schematic diagram of the hM3Dq signaling cascade. Activation of this modified Gq-coupled GPCR (hM3Dq) is achieved by using the DREADD actuator clozapine-n-oxide (CNO) or compound 21 (C21). ACh, the native ligand, is unable to bind to this modified receptor. Binding of the ligand stimulates the calcium signaling pathway, resulting in neuronal excitation.

Chapter 2. Methods

2.1. Ethics declaration

All procedures were approved by the University of Manitoba Central Animal Care Committee (protocol 15-031) prior to commencement, and they were performed in accordance with the guidelines set by the Canadian Council on Animal Care Committee.

2.2. Animals

A total of 24 adult female *Tph2-iCre* (Weber et al. 2011) older than 21 days and weighing 250g-300g were obtained from University of Manitoba (Bannatyne) Animal Care. Initial breeding pairs were kindly donated by the laboratory of Dr. Bartsch and a breeding colony was established here by Central Animal Care Services in 2015. All animals used for this study were females from litters born as offspring in this local colony. The animals were maintained on *ad lib* food and tap water, and automatically programmed 12 hr dark /12 hr light cycles (lights on from 07:00 to 19:00 hr). Rats were mostly housed as 2 rats per cage (25x18x17 cm clear plastic).

2.3. Experimental design

Overall, all experiments reported in this study consisted of the steps outlined in Figure 2.1. On day 0, the selected *Tph2-Cre* rats received hM3Dq-rAAV-complex injections on the right side (n=19), or on left side(n=4), or bilateral (n=1). The recovery period for allowing the expression of the designer receptors in the cell membrane of those neurons that contained Cre varied (22-105 days, see Table 3.1).

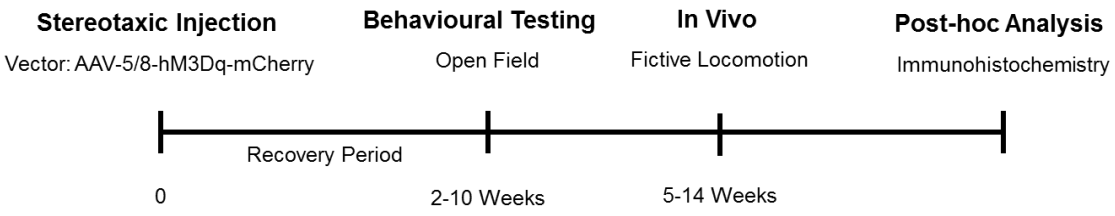

Figure 2.1 Experimental Timeline.
All experiments consisted of an initial recovery surgery during which the Tph2-rats were under isoflurane anesthesia. rAAV-hM3Dq constructs were stereotaxically injected into the PPR, either unilaterally or bilaterally. Rats were allowed at least 2 weeks of recovery time before commencing with behavioral or in vivo experiments. Behavioral testing was done either on 1 day (Series A, see Table 3.1) only or over a period of 27 days with 1-2 trials per week (Series D, see Table 3.1), and not all animals underwent behavioral testing. Terminal fictive locomotor experiments were performed up to 14 weeks after the initial stereotaxic injection. Post-hoc analysis consisted of analyzing data from the fictive locomotor experiments, tissue processing and immunohistochemistry.

2.4. Recovery surgery

At 12-24 hours prior to surgery, Clavamox (Amoxicillin plus Clavulanic acid, 50 mg kg^{-1} day^{-1}) was dissolved in the drinking water as prophylactically to prevent infections related to the surgery. On the day of surgery, the animals were anesthetized with isoflurane (4%) mixed with pure oxygen for 2-3 minutes. After weighing, the animal was transferred to the nose cone for maintenance anesthesia (2%). A surgical plane of anaesthesia was confirmed by the absence of a withdrawal reflex in response to toe pinch. The absence of this reflex was monitored regularly throughout the procedure to confirm maintenance of an appropriate level of anaesthesia. Meloxicam (2 mg kg^{-1}, s.c.), a non-steroidal anti-inflammatory was administered and artificial tears were applied to the eyes. The head was shaved and the surgical site was disinfected three times using chlorohexidine antiseptic, followed by application of 70% alcohol, and 10% povidone iodine, also antiseptic agents. The animal was then transferred to a stereotaxic apparatus (Kopf instruments, Tujunga, CA, USA) where the head was secured with non-puncture ear bars and an anterior mount, ensuring that Bregma and Lamba on the skull remained level.

Temperature was monitored using a rectal thermometer and regulated with a thermostat and a heating pad. Lidocaine (2%) topical gel, a local anaesthetic, was applied to the skin prior to incision. An incision (about 2 cm long) of the scalp was made extending from the eye region to about 1 cm caudal to the Lambda sutures. The bone was scraped clean of connective tissue covering the injection area. The drill (FST 1.4mm, Neurostar) was positioned to touch Bregma and pre-set stereotaxic coordinates were used for the correct placement of the drill with the aid of the rat stereotaxic atlas targeting the PPR which is commonly known as the LPGi (Paxinos&Watson, 2006). The drill was moved to the target coordinates with small adjustments being made based upon skull vasculature (to ensure minimal bleeding while drilling). A 1.7-2 mm deep hole (depending on skull thickness) was drilled through the cranium, using small increments to ensure that the drill bit did not penetrate through meningeal membranes or blood vessels. A 23 gauge needle was then placed within the hole to confirm the absence of bone.

On the stereotaxic frame, the drill was replaced with the injection syringe (Hamilton, 75, SN, 5 µL) loaded with the viral vectors. Beginning at Bregma, the needle was repositioned over the skull and directed to the PPR targets. Once the needle was in place, it was lowered an additional 0.1-0.2 µm then returned back to the injection point. The needle was aimed to target the PPR using stereotaxic coordinates from Bregma (Paxinos & Watson, 2006). By a microinjector syringe pump (Neurostar, GmBh., DE) the viral constructs were injected over 5-7 minutes driven (500-1000 nL). Then the needle was left in place for a few (2-5) minutes following the injection before it was raised slowly from the hole to allow for the tissue to seal and to avoid any potential backflow of the injected vector. In some of the animals, multiple injection tracks rostral or caudal within one opening were used in an attempt to transfect neurons in a larger anatomical region (500 nL per additional injection.)

The skull was washed with sterile saline and the incision was closed with stainless steel surgical clips. To ensure hydration subcutaneous saline was administered (3mL), and after recovery from anaesthesia, the analgesic Buprenorphine (0.5 mg kg^{-1}) was administered. Following the procedure, rats continued to be on Clavamox water for two additional days. The rats were monitored every 8-12 hours initially for successful recovery after surgery, then every 2-7 days thereafter.

2.5. Adeno-associated viral vectors

For the production of the DREADDs, the human muscarinic M3 ion channel, hM3, that is a Gq coupled receptor was cloned. This plasmid was combined with an mCherry c-terminal tag and the human synapsin (hSyn) promoter (provided by UNC Vector core and Addgene). The cre-dependent double floxed open reading frame (DIO) method of re-combination of the hM3Dq-mCherry complex was expected in only those neurons bearing the Cre-recombinase protein. These cells in this animal model are the neurons harbouring tryptophan hydroxylase (Tph2). These constructs were delivered to the neurons by packaging them with recombinant Adeno-Associated Viruses (rAAV, serotype 8 and 5, from UNC Vector Core or Addgene) and injected them to the brain, in the vicinity of the PPR cells. The final vector (5.2 x10E12 for the UNC Vector Core constructs, 4x10E12 for the Addgene constructs genomic copies/ml) was sequenced verified by the manufacturers and then packaged with AAV5/8 serotype coat proteins. Aliquots of viral constructs were stored at -80º C until the day of the surgery, and the thawing and filling of the Hamilton needles occurred at about 2-6 hours prior to the injection.

2.6. Terminal (decerebrate) experiments

Induction of anaesthesia occurred in a plastic chamber using isoflurane 4% in pure oxygen until there was loss of the righting reflex. The animal was weighed and transferred to the dissection table onto a heating pad and placed on a mask. Isoflurane was reduced (2-2.5%) for maintenance and verified by periodically monitoring respiratory rate, blood pressure and heart rate. A pulse oximeter clip was connected to the tail to monitor heart rate and blood oxygenation levels. A rectal temperature probe (coated with petroleum gel) was inserted and a feedback control system was used to keep core temperature between 37-38ºC. Artificial tears were applied to both eyes and the rat was shaved on both hind limbs, on the back from approximately T9-L4 vertebral levels and along the midline of the neck. Lidocaine (2%) gel was applied prior to each incision. Before any surgical procedures, animals were given atropine (0.05 mg kg^{-1} in 2 mL saline and 100 mg dextrose, i.p., 1 mL per side) to reduce secretions and prevent blockage of the tracheal tube.

After checking for the absence of pedal withdrawal reflexes to confirm a surgical plane of anaesthesia, the animal was placed in the supine position for artery cannulation and insertion of the tracheal tube. The left carotid artery was isolated and cannulated (PE 10-20 tubing catheter) for buffer infusion (0.42g $NaHCO_3$ and 2.50 g dextrose in 50 ml nanopure water; 0.9-1.5 mL h^{-1}) and measurement of mean arterial blood pressure (Single-syringe infusion pump, 115 VAC, Cole-Parmer) The muscles along the trachea were gently dissected and a small opening was used for the insertion of a custom tracheal tube, a shortened 20G Hamilton metal needle, for artificial ventilation (Harvard Apparatus Canada, Saint-Laurent, QC, Canada; rate: 60-80 strokes/min; tidal volume range 2.0-2.5 ml) and to monitor expired CO_2 levels (optimally between 3 and 4%).

The rat was rotated back to the prone position for the hind limb nerve dissection. From the top of the femur, an incision was made to the ankle. The biceps femoris muscle was reflected away to expose the sciatic nerve, where the remaining connective tissue was dissected away to expose the distal branches. The tibial (Tib, innervating mainly extensor muscles), the sural (Sur) cutaneous and the common peroneal (CP, innervating mainly flexor muscles) were dissected apart to expose 3-5 mm sections for electroneurogram (ENG) recordings and/or stimulation. Nerves were protected with saline soaked cotton and the incisions were temporarily closed.

The rat received dexamethasone (0.2 mg kg^{-1}) via the carotid artery cannula to reduce potential tissue swelling. The back musculature was bluntly dissected to expose vertebrae T12 to L3 where a laminectomy was performed. The lumbar laminectomy was mainly used to position a cord dorsum electrode for field potential recordings. The exposed tissue and spinal cord was kept moist with saline soaked cotton. The right carotid artery was ligated with a suture (2-0) in preparation for reducing blood loss during decerebration. The rat was then transferred to a stereotaxic frame where the head, vertebrae and legs were secured and immobilized. Ligatures were placed to create pools of warm mineral oil to protect the spinal cord and hind limbs for the rest of the experiment. Isolated nerves were mounted on bipolar electrodes positioned within the mineral oil bath.

Lidocaine gel was applied to the head and then a sagittal incision was made from the base of the nose to the occipital bone. The skin and underlying tissues, including the temporalis muscles were reflected laterally to expose the skull. In order to reduce excess bleeding, the skull vasculature was cauterized prior to skull removal. The bone was removed partially on both sides of the sagittal suture, leaving approximately 1-2 mm margin on each side. Micro-cautery was applied through the skull to reduce excess bleeding from the superior sagittal sinus. A

neuromuscular junction blocker, pancuronium bromide (Pavulon, 0.4 mg kg^{-1}) was administered i.p. in order to prevent any movements during electrophysiological recordings and stimulation periods. The remaining bone around the centre of the skull was removed and the dura was incised in preparation for the removal of the cortices. The decerebration procedure was done by a combination of aspiration and blunt dissection. The cortex was suctioned until rostral colliculi were exposed. At this point, a transection (4 mm posterior to Bregma) was made. All cortex and rostral brain stem regions including the thalamus were removed anterior to the transection. Anaesthesia was discontinued following decerebration after which the animals were ventilated with pure oxygen. The skull was then packed with avitine and/or cotton and the animal was allowed to recover for 45-60 minutes before any further procedure was performed. Electrode placement on the hindlimb nerves (hook, silver electrodes) and Tungsten (TM33B10, World Precision Instruments) microelectrode placement or drug injection needle in the mesencephalon occurred during the recovery time after decerebration. In some animals, an additional opening was drilled at the PPR region by using similar coordinates as during the AAV viral injection. However, in most rats, the original opening from the time of the recovery surgery, thus no additional drilling was necessary.

For MLR-evoked locomotion, using a fine control, hand driven micromanipulator, the tip of the recording electrode was positioned over the head. Based on surface coordinates, the electrode targeted either the rostral edge of the superior colliculus (at an angle of 30-40º, tip caudal) or the border between the superior and inferior colliculus (at an angle of 0-10º). From the surface, the tip was slowly advanced into the midbrain and stimulation was applied while monitoring ENG recordings. MLR stimulation was with square current pulses (20-100 µA, 0.5 ms duration, 18-23 Hz), and the PPR stimulation was the same with intensity varying from 10-

100 µA. Stimulation parameters were adjusted so the locomotor output on the left (L) and right (R) CP and Tib nerves produced rhythmic bursting.

The cord dorsum potential electrode (CDP) was used to test responses to hind limb nerve stimulation as a means to establish the baseline state of the lumbar spinal cord. Hind limb nerves were stimulated in multiples of the intensity required to activate the most excitable fibres, called threshold (T), normally at intensities of 5 times threshold (with 1-4 pulses, at 200 Hz). The ENGs and the blood pressure recordings were continuously monitored and recorded.

2.7. Drugs used to activate the designer receptors

Clozapine-n-oxide (CNO, Abcam, USA) was dissolved in sterile saline and it was injected intraperitoneally (i.p.) for behavioral procedures (dose 0.3 mg kg^{-1}). During the fictive locomotion studies, CNO was injected via the arterial blood pressure monitoring pump (dose of 0.3-1 mg kg^{-1}) or applied by pressure injections intracerebrally. For the intra cerebral injections, a 50µM solution was used in doses of 500 nL with 1-4 applications per animal.

Compound 21 is an alternate actuator for hM3Dq. It is only cited in one publication (Chen et al. 2015); therefore, it was difficult to design its best dosing for this study. We opted for similar dosages as the CNO injections used in these animals (i.e. tests prior to obtaining C21). Only intraperitoneal application of C21 was done here during both the open field behavioural and the fictive locomotor tests.

Since systemically injected CNO has recently been shown to be back-metabolized to clozapine in rats (MacLaren et al. 2016; Gomez et al. 2017) it was decided to use clozapine was used during behavioural testing . This information was only known in the second series of tests,

not in the first series. The clozapine was tested at similar doses to the CNO, 0.3 mg kg^{-1}, in order to evaluate the effects that might have been related to clozapine rather than CNO.

2.8. Electrophysiological data acquisition and analysis

Electroneurograms (ENGs) were amplified (5-10,000 times), analog filtered (30 Hz – 3 kHz) and digitized (at 500 Hz – 20 KHz sampling rate). Custom-made capture and analysis software was used to record signals and the Analysis software was used for post-hoc data processing and analysis. Both packages were developed and customised by G. Dettilieaux in the Spinal Cord Research Center, University of Manitoba (see more documentation at www.scrc.umanitoba.ca).

Fictive locomotion was initially analysed by first determining the number of nerves in each animal with rhythmic activity. Then the rhythmic bursts were analysed by first selecting an episode of repetitive bursts lasting for at least 20 seconds. The onset and offset of the bursts were determined by a threshold crossing algorithm automatically and sometimes adjusted manually by visual inspection. As illustrated in Fig. 2.2, the burst duration (time between onset and offset of ENG bursts) or the cycle duration (time between onset and subsequent burst onset of flexor or extensor bursts) was calculated after exporting the set values from Analysis into Microsoft Excel (Windows 10).

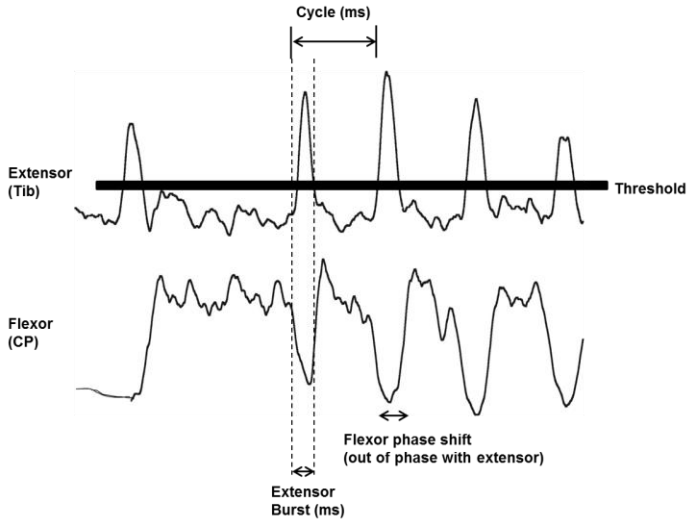

Figure 2.2 Analysis of burst duration (ms), cycle duration (ms), and phase shifts from ENG data.

Intralimb ENG data illustrating a pattern of alternating extension and flexion from the tibial (Tib) and common peroneal (CP) nerve. In order to be selected as a burst, the ENG trace amplitude must cross a chosen threshold level thus eliminating non-biological activity (noise) from burst selection. Cycle period (ms) is defined as the time between the onset of two successive extensor or flexor bursts (ms). Burst duration is defined as the time between onset and offset of ENG busts. Coordination, or alternation of flexor and extensor nerves is measured by the phase shift between two subsequent ENG bursts.

Spontaneous hindlimb nerve activity was also evaluated by noting and counting the bursts (either tonic or rhythmic) on each of the tested hind limb nerves when ENG activity was apparent in the absence of any brain stimulation.

2.9. Rat behavioural (open field) assessment in awake, conscious animals

All behavioural procedures were conducted during the light portion of the light-dark cycle, between 9 and 16 hours. Animals received at least two acclimatization sessions with the test box and the experimenter handling prior to the first trial day. The open field arena was 1.25 m x 0.61 m, and divided into eight segments (6 L, 2 W) for analysis which was approximately one rat's length.

The procedure for the initial eight animals (Series A) was the following: animal was placed in the open field box for ten minutes to measure baseline activity. Then, the animal received a saline injection (0.3 ml, i.p.) and was allowed to rest in its home cage for 2 minutes. Then the animal was placed back in the box for 15 minutes. After this period, the animal was injected with CNO (0.3 mg kg^{-1}, i.p.) and placed into the open field for 30 minutes. The open field box was cleaned with Oxivir plus, a disinfectant (1:40 dilution), after each trial.

In the second paradigm (Series D) the animals received one acclimatization training period. For this series, animals were placed in the box for ten minutes. Then animals received either saline (0.3 ml, i.p.) or drug (CNO, clozapine or C21) and placed back in the box for an additional 50 minutes initially, but after two trials this time was reduced to 15 min due to the lack of any activity beyond this time point.

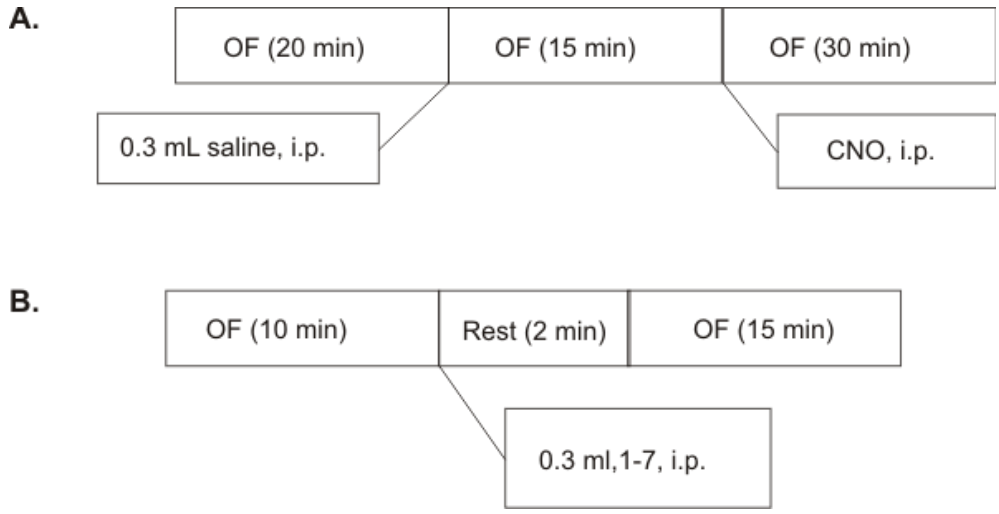

C.

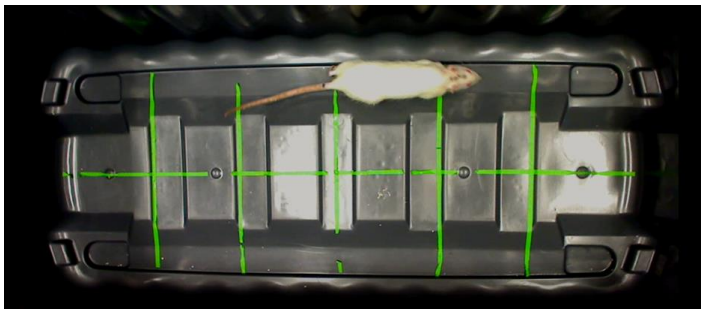

Figure 2.3 Protocol for behavioural analysis.

- **A.** In series A, during the behavioural protocol, animals were placed in open field (OF) to test locomotion, grooming and rearing activity. Then, they were injected with 0.3 ml saline, i.p., and placed back in the box for 15 minutes for continued open field testing. Subesequently, they were given an i.p. injection of CNO (0.3 mg kg^{-1}) and placed back into the box for an additional 30 minutes. This was repeated twice with a 7 day interval between the two open field testing sessions
- **B.** In Series D, the behavioral testing took place over a total time of 25 days (sessions 1-7). The rats were placed in the open field for 10 minutes, then removed from the box and injected 0.3 ml, i.p. of a compound dependent on session number. The sessions occurred in this order: 1-Saline baseline; 2-Saline baseline; 3- Compound 21 (0.3 mg kg^{-1}); 4-CNO (0.3 mg kg^{-1}); 5-Clozapine (0.3 mg kg^{-1}); 6-Saline/DMSO baseline; 7- Compound 21 high dose (1 mg kg^{-1}). There were 3-6 days between behavioral sessions (4, 4, 5, 6, 3, 3 days between sessions 1-7, respectively).
- **C.** Video recording from open field chamber demonstrating the arrangement of the open field (6 squares long by 2 squares wide).

All behaviors were videotaped and scored by two experimenters. The parameters were quantified from the recordings and analyzed as follows: the locomotor score was calculated by counting the number of lines in the box (within the 6x2 matrix); the rearing was evaluated by counting the number of episodes when the rat's front leg was not in contact with the ground (either without support in the air or resting on the side of the box); and the episodes of grooming were measured by counting the occurrence of the rats scratching, biting or licking their skin or cleaning their face with the fore paws. Only locomotor results will be reported below.

2.10. Immunohistochemistry and microscopy used on brain and spinal tissue

All animals were perfused in a fume hood after fictive locomotion experiments with 30 mL pre-fix wash (0.9% saline solution and 0.5% heparin) followed by an ice-cold fixative (4% paraformaldehyde (PFA) in 0.1 M phosphate buffered (PB) solution. Brainstem and some spinal cord segments were removed and placed in PFA overnight. These tissue sections were immersed in graded sucrose solution (20% after 24 hours, 30% after 48 hours) with 0.1 M phosphate buffer and were stored at 4ºC until sectioning. Brainstems were coronally sectioned (20-25 µm) using a cryostat (CM3050 S, Leica Microsystems, Heidelberg, Germany). Sections were collected in a multi-well plate containing 0.500 µL of 0.1M phosphate buffer (PBS). Every 300 µm, one section was collected on a coated slide to visualize the native mCherry protein. Slides were cover slipped with fluormount-G (Southern Biotech). Floating tissue was transferred into 0.1 M PBS solution with 0.1% sodium azide and stored at -20ºC in an ethylene glycol cryoprotectant solution.

To perform free-floating immunohistochemistry, sections were washed three times for ten minutes each in 0.1 PBS. The fourth wash was by placing them in a blocking buffer (0.3% Triton X-100, normal donkey serum and 0.1 PBS) for at least one hour. Primary and secondary antibodies were diluted in the same blocking solution. Sections were then placed in blocking solution and primary antibody overnight at 4ºC. Then, these sections were incubated in the secondary antibodies for 2 hours at room temperature and later washed again (three times for 10 minutes, in 0.1 PBS). Seven to ten sets of serial sections were then mounted on gelatin-coated slides and they were cover slipped with fluoromount-G (Southern Biotech). The primary antibody was NeuN (Abcam, USA, 1:500).

The processed slides were visualized under a Zeiss semi-automated; fluorescent microscope (Axioscope 2, Zeiss or Zen 2.3 Blue edition, Zeiss) and images were taken with an AxioCam camera and the AxioVision or the Neurolucida software's. The filters that were used to visualize the reporter m-Cherry protein were optimized for Texas red or Cy3 (561-594 nm or 548-561 nm, respectively). The images were imported into Corel DrawX4 program without further editing or changes made to the background or image colour intensity.

Chapter 3. Results

Table 3.1illustrates either behavioural data (15/24) or fictive locomotor data (16/24) obtained from the listed animals or both behavioural and fictive locomotor data from the same animals (11/24). The rats lost before data collection included one due to drop in respiratory and heart rate during magnetic resonance imaging, two due to blood loss during decerebration before MLR stimulation was commenced, and two in which no hind limb ENGs could be evoked in a repeatable manner. **Series A** included the animals that received viral vectors from UNC vector core and that had received systemic CNO. **Series B** included animals that were injected with viral vectors from Addgene and also received systemic CNO. These two viral vector constructs are seemingly identical; the only difference is the supplier and viral titer. **Series C** received viral vector injections from Addgene, but had received localized intracerebral injections of CNO during the in vivo experiment, plus some of these animals also received C21systemically, that comprise experiments for **Series D**.

As indicated in Table 3.1 not all data is available (n/a) as in the case of some animals have completed the behavioural studies but not yet the decerebrate experiments or some of the brain tissue post-hoc analysis is still incomplete (i.e. n/a in the m-Cherry column). Brain tissue from all animals have been collected for verifying the presence of the reporter protein associated with the designer receptors (m-Cherry) and tissue from 19/24 rats have been processed to date. The simultaneous PET/fMRI imaging results were added in Appendix A as the involvement in those experiments was relatively large with respect to the time and procedural complexity.

Animal ID#	In vivo exp #	AAV days	AAV Supplier and Serotype #	In vivo CNO	C-21	MLR + PPR	Spont pre/ post	Behav.	m-Cherry	PET-MRI
Series A; Systemic CNO										
1965	55	77	UNC; 8	null				+	+	+
1966	56	71	UNC; 8	0.3		+	+/-	+	+	
1967	58	77	UNC; 8	0.5		+	-/-	+	+	
1981	63	85	UNC; 5	0.5		+	+/+	+	+	+
1978	59	73	UNC; 8	1		+	-/-	+	+	
1979	61	85	UNC; 8	1		+	+/+	+	+	+
1989	62	85	UNC; 5	1			-/-	+	+	+
1990	60	77	UNC; 5	1		+	-/+	+	+	
2624	64	92	UNC; 5	null					+	+
2625	65	104	UNC; 5	1		+	+/+		+	+
Series B; Systemic CNO										
9218	68	84	Addgene; 8	0.3		+	+/-		+	
9219	69	91	Addgene; 8	null					+	
9220	71	105	Addgene; 8	0.3		+	-/+		+	
8985	73	86	Addgene; 8	0.3		+	-/+		+	
8987	72	77	Addgene; 8	0.3		+	-/+		-	
8988	70	64	Addgene; 8	null					+	
Series C; Intracerebral CNO and Series D; Systemic C21										
8986	74	105	Addgene; 8	50nL x 3			-/+		+	
14381	75	20	Addgene; 8	50nL x 3	0.3		-/+	+	+	
14382	76	27	Addgene; 8	null	0.3			+	+	
14773	77	34	Addgene; 8	50nL x 3	0.3		+/+	+	n/a	
14774	78	48	Addgene; 8	50nLx 4	0.3 x 2		-/+	+	n/a	
14398	n/a	n/a	Addgene; 8	n/a	n/a			+	n/a	
14399	n/a	n/a	Addgene; 8	n/a	n/a			+	n/a	
14400	n/a	n/a	Addgene; 8	n/a	n/a			+	n/a	

Table 3.1 Description of experimental series

The columns (from left to right) indicate: 1 - animals identification number, 2 – in vivo experiment number, 3 – total amount of AAV transfection days, 4 – AAV supplier and serotype, 5 –dosage of CNO (mg kg^{-1}) for and the volume of CNO for intracerebral injections (multiples of 50nM, 500 nL injections during experiments) 6 – dosage of C21 (mg/kg) for systemic injections 7 – combined MLR and PPR electrical stimulation, 8 – spontaneous hindlimb nerve activity either pre and/or post designer drug application systemic compound 21 administration and 9 – Behavioral (open field) experiments, 10- presence of the reporter protein for DREADDs as identified by post-hoc tissue analysis of the brain. The + represents that the animal underwent the respective experimental procedure, the – indicates absence of effect (spontaneous activity). Tissue processing has not been completed for animal #14773 and #14774 and therefore has been denoted as n/a. The animals with no in vivo data are denoted as null.

3.1. Electrical stimulation of the PPR in adult rats enhances MLR-stimulation induced locomotion

The purpose of these experiments was to characterize the effects of electrical stimulation applied to the PPR in adult rats in combination with electrical stimulation of the MLR. The animals from which data was obtained were from two cohorts, referred to as series A and B (see Table 3.1). Series A consisted of one group (n=8) with viral constructs from UNC Vector Core either with AAV8 serotype (n=5) or AAV5 serotype (n=3). Series B had viral constructs manufactured by Addgene with AAV8 serotype (n=4).

In these experiments, the data was analysed investigating how fictive locomotor activity induced by MLR stimulation was modified when PPR stimulation was concomitantly applied. In some rats, MLR stimulation alone did not elicit locomotion as defined by alternating flexor and extensor hindlimb nerves with rhythmic ENG bursts lasting for 20s or longer. For example, the bout of activity shown in Fig. 3.1A exemplifies tonic activity in 2/4 nerves and no or low level tonic activity in the other two nerves in this animal. Changes in this type of tonic activity after adding the PPR stimulation was evident as illustrated in Figure 3.1B. Note the changes in the amplitude of the tonic bursts and the changes from tonic activity to rhythmic bursting in both the flexor and extensor ENGs.

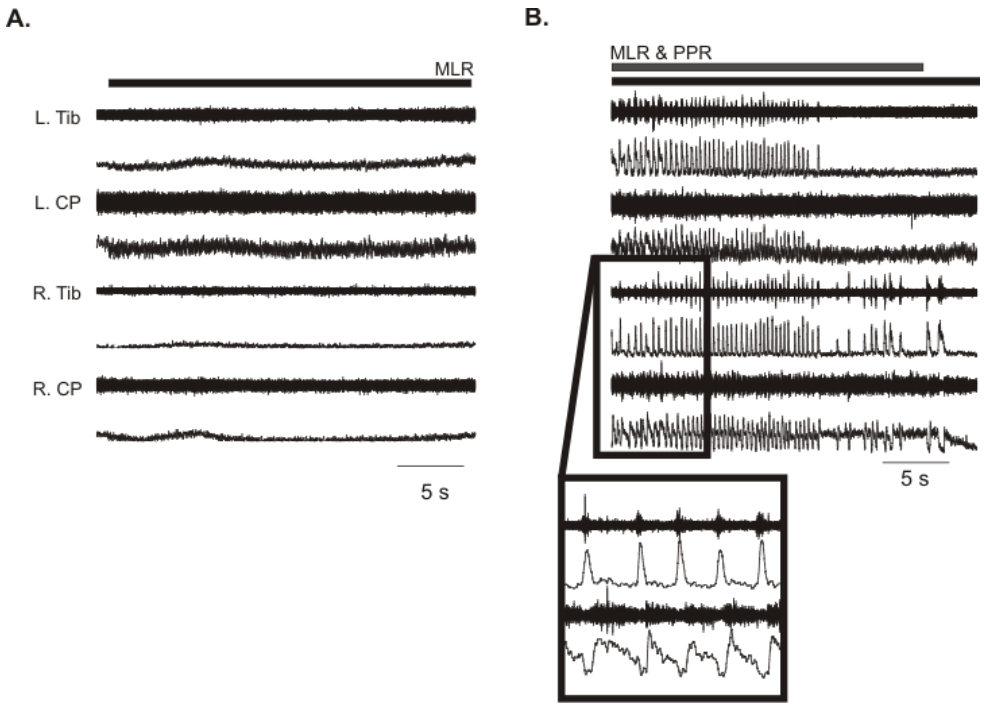

Figure 3.1 PPR facilitates MLR-induced tonic activity
Fictive motor activity resulting from mesencephalic locomotor region (MLR) stimulation was monitored recording: raw ENG traces (top) and those were amplified, filtered and rectified (bottom).

- **A.** During MLR stimulation (80 µA, black bar), MLR did not elicit bursts in any of the nerves. Only left (L) CP displayed tonic activity during the MLR stimulation.
- **B.** ENGs in the same rat following stimulation in the PPR (30 µA, gray bar) added to MLR stimulation. Activity is induced in all four nerves and it is locomotor-like as there is alternation between flexor and extensor nerves (as shown in outset box illustrating 2 seconds of R.Tib and R.CP alternation).

As illustrated in Fig. 3.1A-B motor activity from a rat in series A with an AAV5 construct from UNC. Two other rats in this series injected with the same viral constructs failed to show rhythmic activity upon MLR stimulation. Furthermore, PPR stimulation in combination with MLR stimulation did not notably facilitate ENG activity. The presence of the m-Cherry reporters, however, was verified in all three rats, as shown in Fig. 3.2.A, B and C. The m-Cherry containing cells were confirmed to be neurons (NeuN positive cells).

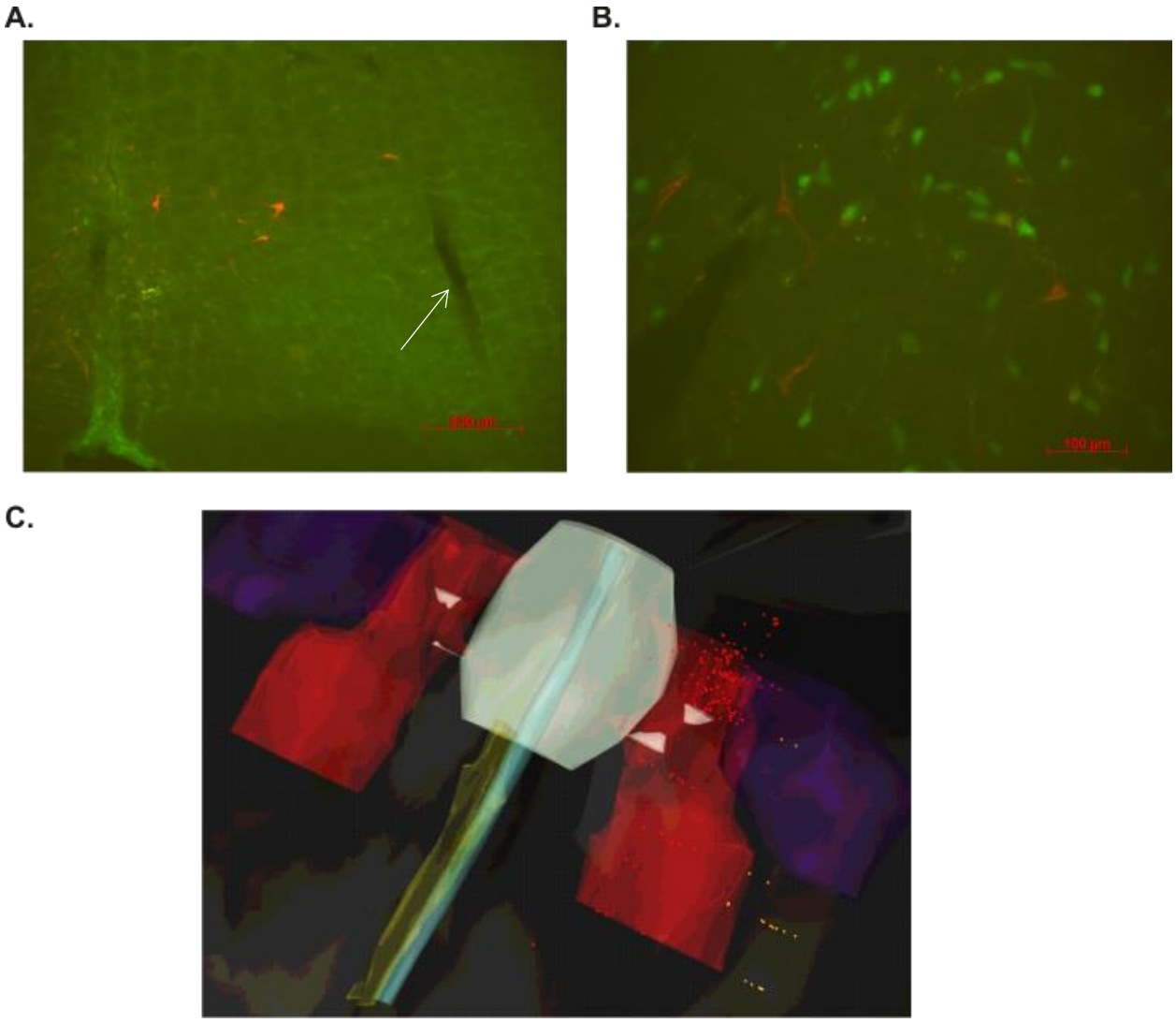

Figure 3.2 Immunohistochemical verification of m-Cherry reporter in the PPR

- **A.** Coronal section from *Tph2-Cre* rat injected with AAV5 serotype viral constructs showing the presence of the reporter protein, mCherry (red) that has been tagged to the hM3Dq (scale bar 500 µm). Arrow indicates location of PPR electrode.
- **B.** Coronal section from *Tph2-cre* rat injected with AAV5 serotype viral constructs showing the presence of the reporter protein, mCherry (red) and NeuN, neural marker protein (green) (scale bar 100 µm).
- **C.** Reconstruction of mCherry (red dots) positive cells from sections collected every 200µm apart and by identifying markers for the different levels of the reticular formation (i.e. cranial nucleus of the 7th nerve (purple) the raphe magnus (light green) the raphe pallidus (darker green), rostro-caudal extent of the LPGi (red).

In cohort B, 0/4 rats showed alternating activity on all four hind limb nerves but 4/4 showed rhythmic activity at least on one nerve, the R. CP, as illustrated in Figure 3.3. In this rat, the MLR stimulation alone also induced rhythmic activity in R. Tib that was not altered by PPR stimulation. Neither was the tonic MLR-induced L. Tib and L. CP output altered by the PPR stimulation.

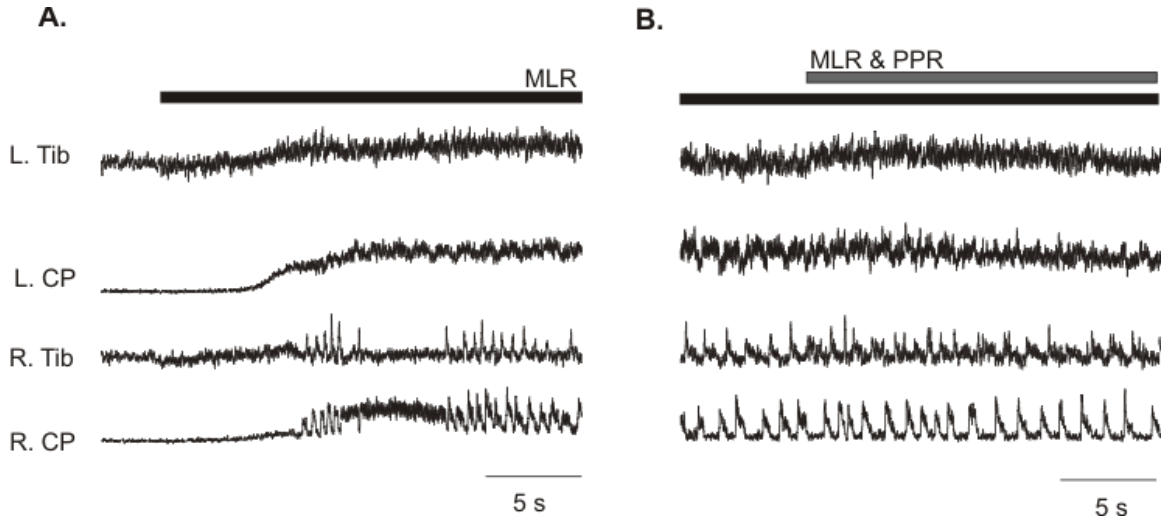

Figure 3.3 PPR facilitates MLR induced alternating flexor-extensor activity.
Hindlimb ENGs from flexor (CP) and extensor (Tib) nerves on the right (R) and left (L) following electrical stimulation of the mesencephalic locomotor region (MLR). Rectified and filtered ENG traces are displayed. MLR stimulation is denoted by the black bar and PPR stimulation is denoted by the gray bar.

- **A.** During MLR stimulation (75 µA) there was an initial delay for the onset of activity. The L.Tib and L.CP nerves remained tonic. The R.Tib and R.CP exhibited both tonic activity and bursting type of activity.
- **B.** When PPR stimulation was added during the same trial, longer bursts were evident in both the R.Tib and R.CP nerves while the activity did not change in the L.Tib or L.CP nerves.

When MLR stimulation evoked rhythmic activity in at least one of the recorded hindlimb nerves, such as the bout illustrated in Fig. 3.4, it was feasible to compare changes in the rhythmicity of the bursts before and after the PPR stimulation was added. This example illustrates that bursts increased in amplitude and a longer bout of rhythmic bursting could be

evoked by combined MLR and PPR stimulation than with MLR stimulation alone. The R.CP burst durations in this case increased from 131±25ms to 175±31ms.

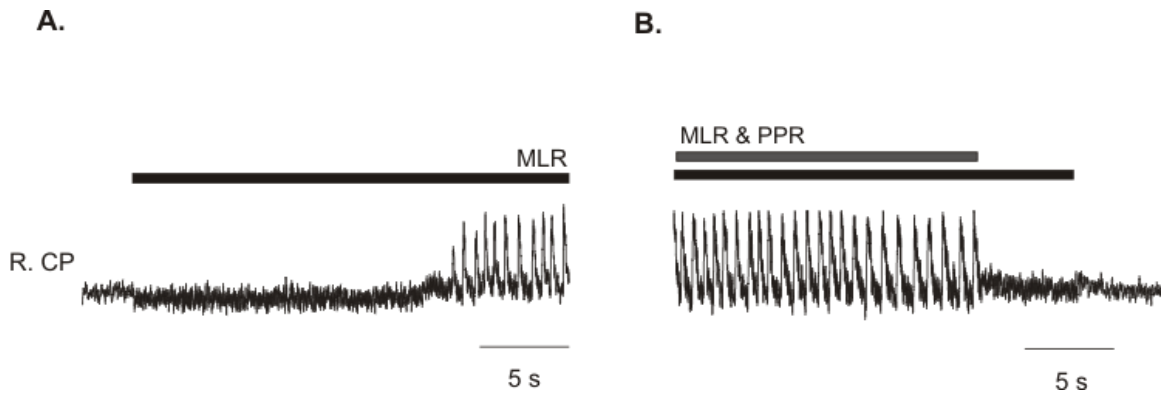

Figure 3.4 MLR with PPR stimulation facilitates flexor nerve burst frequency and amplitude.

Hindlimb rectified and filtered ENG recordings from R.CP. No nerve activity during stimulation was detected in the other three nerves and therefore they have been excluded. The black bar represents when MLR stimulation was turned on.

- **A.** During MLR stimulation (40 µA), rhythmic bursting is induced in the R. CP.
- **B.** When combined MLR stimulation and PPR (30 µA) stimulation was used, R.CP exhibited a greater amplitude and faster burst frequency than during the "MLR only" stimulation.

Overall, the rhythmic activity on the R.CP nerve before and after PPR stimulation could be examined in 6 rats from cohort A and B. The summary of these results is shown in Fig. 3.5. In all but one of the 14 bouts analysed from the 6 rats, there was an increase of R.CP burst duration, as shown in Fig. 3.5A. On average, the R.CP bursts increased to 174±98% (s.d.) of the burst duration evoked with only MLR stimulation applied. The absolute cycle durations were variable; on average, they ranged from 100 ms to about 800 ms. After removing 2/15 bouts with very high bursts durations of over 2000 ms, resembling tonic activity, the graph in Fig. 3.5B illustrates that the absolute R.CP bursts increased in all but one tested bout. When comparing the average burst durations with and without PPR stimulation with a paired t-test, there was a statistically significant increase from 287 to 417 ms ($p=0.01$).

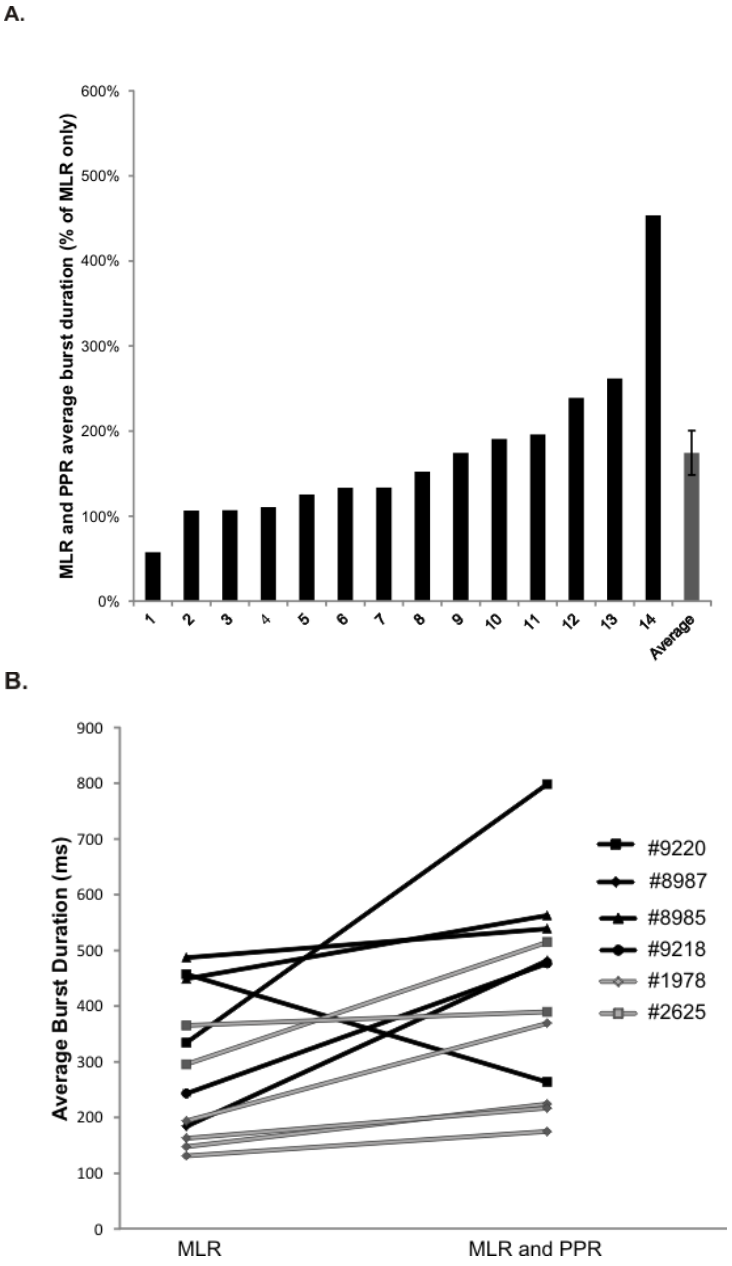

Figure 3.5 Average burst duration in the common peroneal nerve increased with PPR stimulation.

A. Burst durations were averaged during MLR stimulation (over a 30 s bout) and during MLR and PPR stimulation (also over 30 s) in each animal from series A (gray-see table 3.1) and from series B (black). The R.CP burst durations during PPR & MLR stimulation expressed as % of the R.CP bursts during MLR stimulation in each bout (2-4 bouts per animal) (sorted in ascending order). The error bar on the average represents standard error of the mean.

B. Paired absolute burst durations (ms) during MLR stimulation (on the left) and during MLR and PPR stimulation (on the right) in the same rat.

3.2. Selective stimulation of the PPR neurons in adult rats harbouring DREADDs by systemic CNO administration

The purpose of these experiments was to characterize the effects of serotonergic neural stimulation within the PPR in adult rats. Alternating rhythmic activity on four hindlimb nerves was not evoked by MLR stimulation alone as a baseline prior to the CNO administration in series A and B, thus the effects of CNO application could not be evaluated. There were 4 rats (1/7 in cohort A and 3/4 in cohort B) with two or more rhythmic hindlimb nerve with MLR stimulation prior to CNO administration. In most of these animals, the relationship between burst durations and cycle durations could be analysed before and after CNO injections and there were no differences in their response (data not shown). The time required for MLR stimulation to evoke tonic activity in each of the nerves was also assessed before and after CNO injections. There was a trend but not significant shortening of this time after CNO injections (data not shown). One common observation in all series was that the ENG activity evoked by a set current intensity of MLR and/or PPR before CNO administration could be evoked by a lower intensity stimulation of the MLR and/or PPR after CNO.

Another typically observed pattern was that the efficacy of PPR stimulation to trigger rhythmic ENG output was lost over time after CNO. In some cases, both the MLR and the PPR stimulation had become ineffective in generating any motor output in spite of robust effects evoked prior to CNO application. The loss of evoked motor activity by combined MLR and PPR stimulation is illustrated in Fig. 3.6. These are bouts from the same animals that were used in Figs. 3.1, 3.2 and 3.3 illustrating the effects of PPR stimulation prior to CNO injections. The bouts shown in Fig. 3.6A, C and E were taken post CNO injections at 19, 3 and 1 minute, respectively, when the electrical brain stimulation was still relatively effective in generating

rhythmic, locomotor-like ENG activity. The bouts shown in Fig. 3.6B, D and F were taken at 67, 12 and 20 min, respectively, post CNO injection when stimulation induced only tonic activity (in Fig. 3.6B) or nearly zero activity (in Fig 3.6D,F).

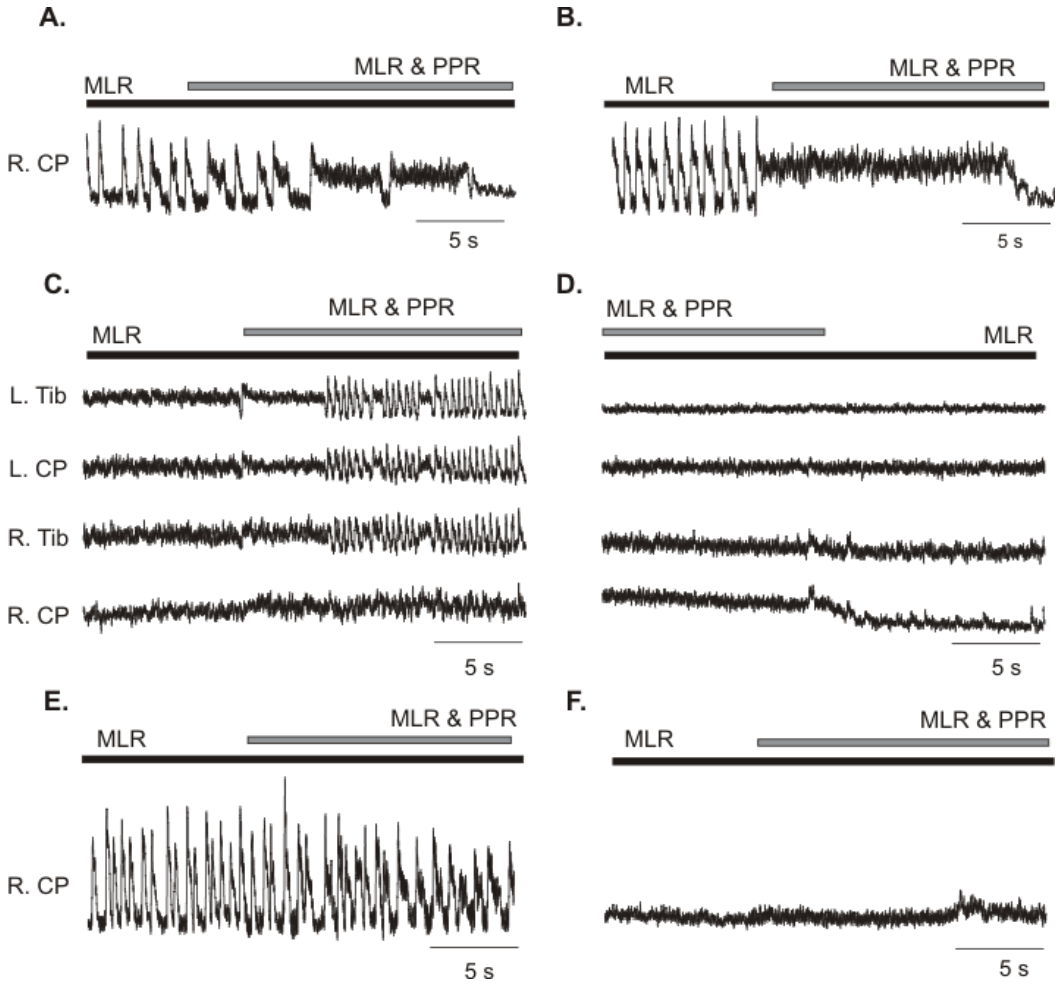

Figure 3.6 Change in rhythmicity after systemic CNO administration.
Rectified and filtered ENG recordings from the indicated hindlimb nerves during MLR (black) and PPR (gray) stimulation (as indicated by the stimulation bars) at different times following systemic CNO injections (0.3-1 mg kg^{-1}).

- **A.** Rat from series A, serotype 8, 19 minutes and
- **B.** 67 min after CNO.
- **C.** Rat from series A, serotype 5, 3 minutes and
- **D.** 12 minutes after CNO.
- **E.** Rat from series B, serotype 8, 1 minute and
- **F.** 20 minutes after CNO.

3.3. Selective stimulation of the PPR neurons in adult rats harbouring DREADDs by intracerebral CNO

The intracerebral injections of CNO (500 nL boluses of 50 nM) were intended to target the same brain regions as during the delivery of the AAV-DREADD complexes. They were administered to reduce the confounding effects of CNO when applied systemically. These were attempted successfully in 4 animals. As described in section 3.2, the analysis of the CNO effects was dependent upon the type of ENG activity that was elicited by MLR stimulation. The number of active nerves and the type of activity (tonic vs. phasic) was different in the tested animals. In all animals, however, it was verified that the same type of ENG activity that was typically elicited by a set MLR site with a set current intensity could be evoked by less current (i.e. MLR stimulation intensity) after CNO application.

Due to the variable activity in the tested nerves pre and post CNO, only 2/4 animals that had both flexor and extensor activity before and after CNO were evaluated in terms of the locomotor-related actions of intra-cerebral CNO injections. The examples in Fig.3.7 show polar plots comparing the onset of extensor (Tib) and flexor (CP) ENG activity during locomotion induced by mesencephalic locomotor region (MLR) stimulation in these 2 rats. The polar plots, specifically the dots around the circles, represent the phase shift expressed in degrees (0-360 degrees) between the two nerves compared; in this case a flexor and an extensor. The phase shift, or the time between the onset of the flexor and the extensor nerve in each of the bursts observed during the analyzed bout of activity is shown from one animal (Fig. 3.7A) on the right side and from the other animal with comparing nerves on both sides (right Fig.3.7B and left Fig. 3.7C). The expected phase shift is 180 degrees when a flexor and extensor nerve is alternating. In the top row (Fig. 3.7A1, B1 and C1) most bursts are close to this expected value. After intracerebral

injections of CNO, however, changes in the flexor and extensor relationship show that the averages were reduced: the average values shifted to near zero (or 360 degrees) in both animals.

The length of the black line in each circle is an indicator of statistical significance of the detected coupling, the **r**-value. If the line crossed the confidence interval (the dotted line, 95% interval) then the two nerves have a phase-coupled relationship i.e. not randomly bursting in a phasic manner. Before CNO, the **r** values were 0.90, 0.95, and 0.75 (A1, B1, C1 respectively). Then 0-10 minutes after CNO, the all **r** values were to 0.97, 0.95, 0.80 (A2, B2, C2 respectively); and later by 20-40 min post CNO the **r**-values were 0.832, 0.91, 0.78 (A3, B3, C3 respectively).

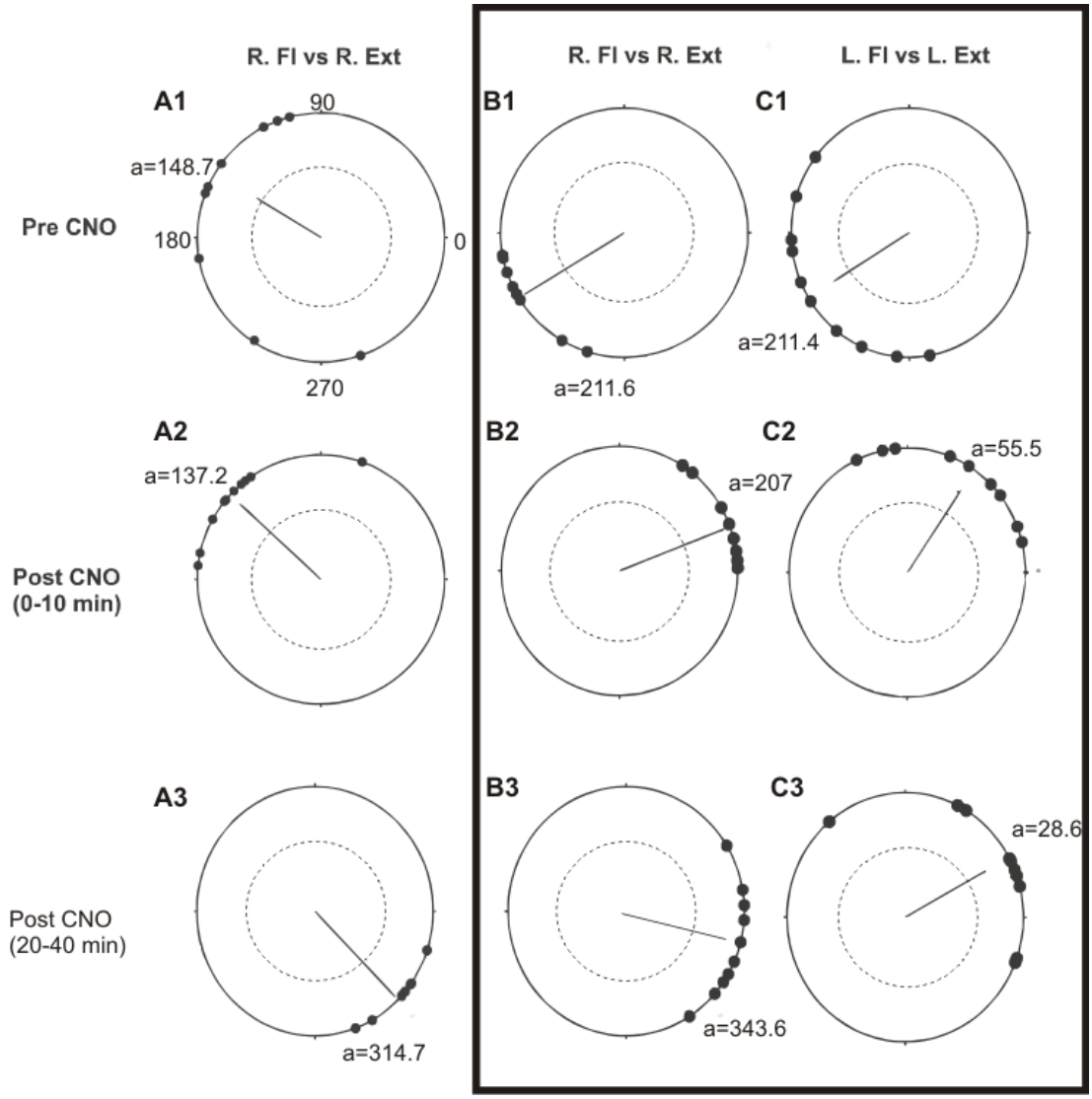

Figure 3.7 Intra-limb coordination after intracerebral CNO.
Polar plots of the phase relationships between the onset of Tib burst activity and the CP activity quantifying intralimb coordination. The 0 position on the polar plot corresponds to the onset of ENG activity in the TA nerve, and the filled circles (black, each representing a burst from the bout of 10 consecutive steps) indicate the onset of activity in the CP nerve in the same limb. The black bar in all circles demonstrates the average phase shift (as an angle between 0 and 360 degrees, and the length of the bar is a measure of the strength of this relationship, the r value).

- **A.** One rat with right (R.) flexor and extensor coupling prior to intracerebral CNO injections (A1) and at 8 minutes (A2) and later at 20(A3) minutes after that.
- **B.** One rat with right (R.) flexor and extensor coupling prior to intracerebral CNO injections (B1) and at 9 minutes (B2) and later at 40 (B3) minutes after that.
- **C.** Same rat as B with left (L.) flex and extensor coupling prior to intracerebral CNO injections (C1) and at 9 minutes (C3) and later at 40 (C3) minutes after that.

3.4. Changes in spontaneous fictive motor activity after chemogenetic stimulation of the PPR neurons

The decerebrate rat preparations could exhibit tonic and/or locomotor-like fictive hindlimb activity even in the absence of MLR or PPR stimulation. Such episodes of spontaneous activity when there was no external trigger or stimulus applied to the animal was evaluated with respect to the frequency of their occurrences and the type of ENG activity that was apparent during these episodes. As shown in Table 3.1, spontaneous activity was observed in all three series. A spontaneous bout is defined as the initiation of ENG activity in the absence of spontaneous activity. These spontaneous bouts usually occurred between two episodes of brain stimulation sessions when no external stimulus was applied however, the ENG activity was still recorded with the data capture system. One key feature of these episodes is that they were highly variable, as exemplified by the illustrations in Fig.3.8. The panels in Fig 3.8A show that spontaneously evoked tonic activity as well as rhythmic bursts could manifest on different hindlimb nerves as shown in Fig. 3.8C even prior to chemogenetic stimulation. After systemic CNO application, spontaneous episodes did not change in terms of ENG profiles as shown by the example in Fig. 3.8B, while in other cases, the frequency of the burst changed as in Fig.3.8D, E and F.

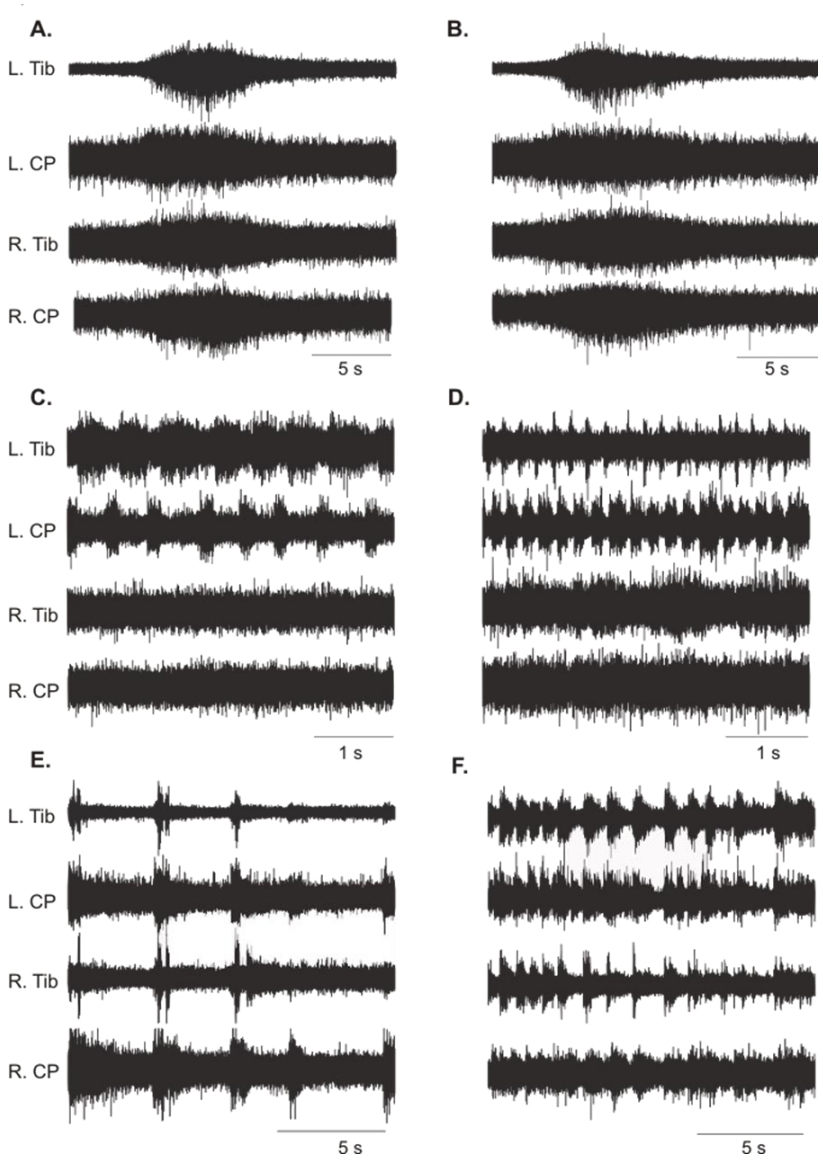

Figure 3.8 Spontaneous activity is variable among drug application paradigms.
Raw ENG recordings from the indicated hindlimb nerves.

- **A.** Spontaneous activity in a rat from Cohort A before systemic CNO.
- **B.** Spontaneous activity in a rat from Cohort A 4 minutes after systemic injection of CNO
- **C.** Spontaneous activity from Cohort C before intracerebral CNO
- **D.** Spontaneous activity from Cohort C 35 minutes after intracerebral CNO
- **E.** Spontaneous activity from Cohort D after intracerebral CNO (1h43 min) and before systemic injection of C21
- **F.** Spontaneous activity from cohort D 1h30 min after systemic C21.

In series C and D with intracerebral CNO injections and systemic C21 application, the frequency of spontaneous activity was determined. Recordings from one of these animals in Fig. 3.10A-D illustrates that the type of spontaneous activity changed after both intracerebral CNO and systemic C21 injections. Such qualitative changes were not analyzed here but they could be informative and it is possible to extract such data from the collected bouts. Quantitatively, the overall occurrences of spontaneous activity before and after CNO administration are summarized in Fig 3.9.

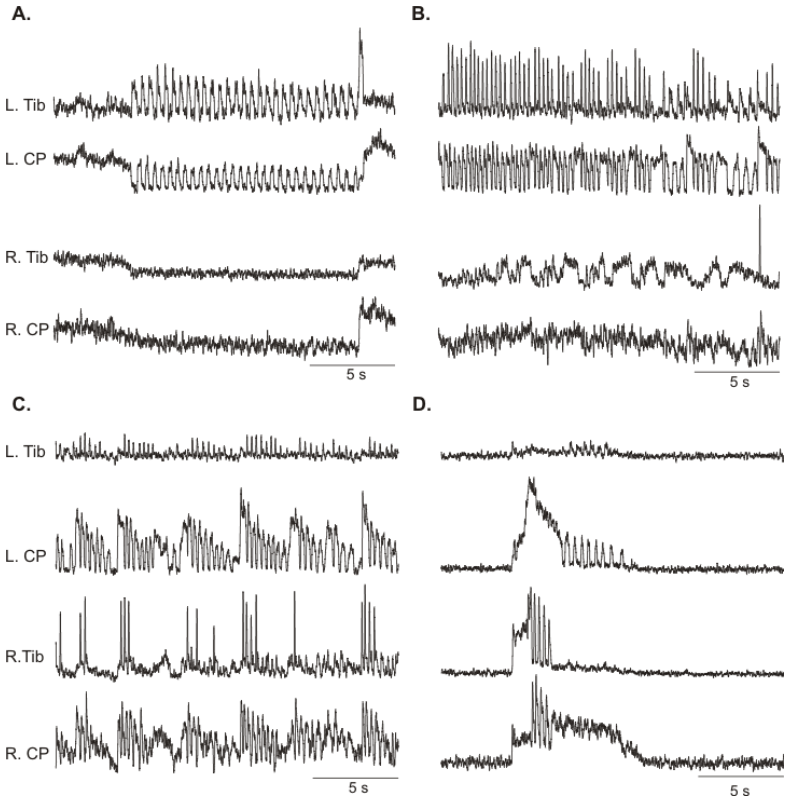

Figure 3.9 Instances of spontaneous activity in cohort D after intracerebral CNO and systemic C21

- **A.** An example of spontaneous activity in animal #14773L before intracerebral CNO.
- **B.** Same rat as in B, with spontaneous activity 35 minutes after the first intracerebral CNO.
- **C.** Same rat as in B and C, spontaneous activity 75 minutes after the first intracerebral CNO but pre C21.
- **D.** Same rat as in B – D, spontaneous activity 11 minutes after C21.

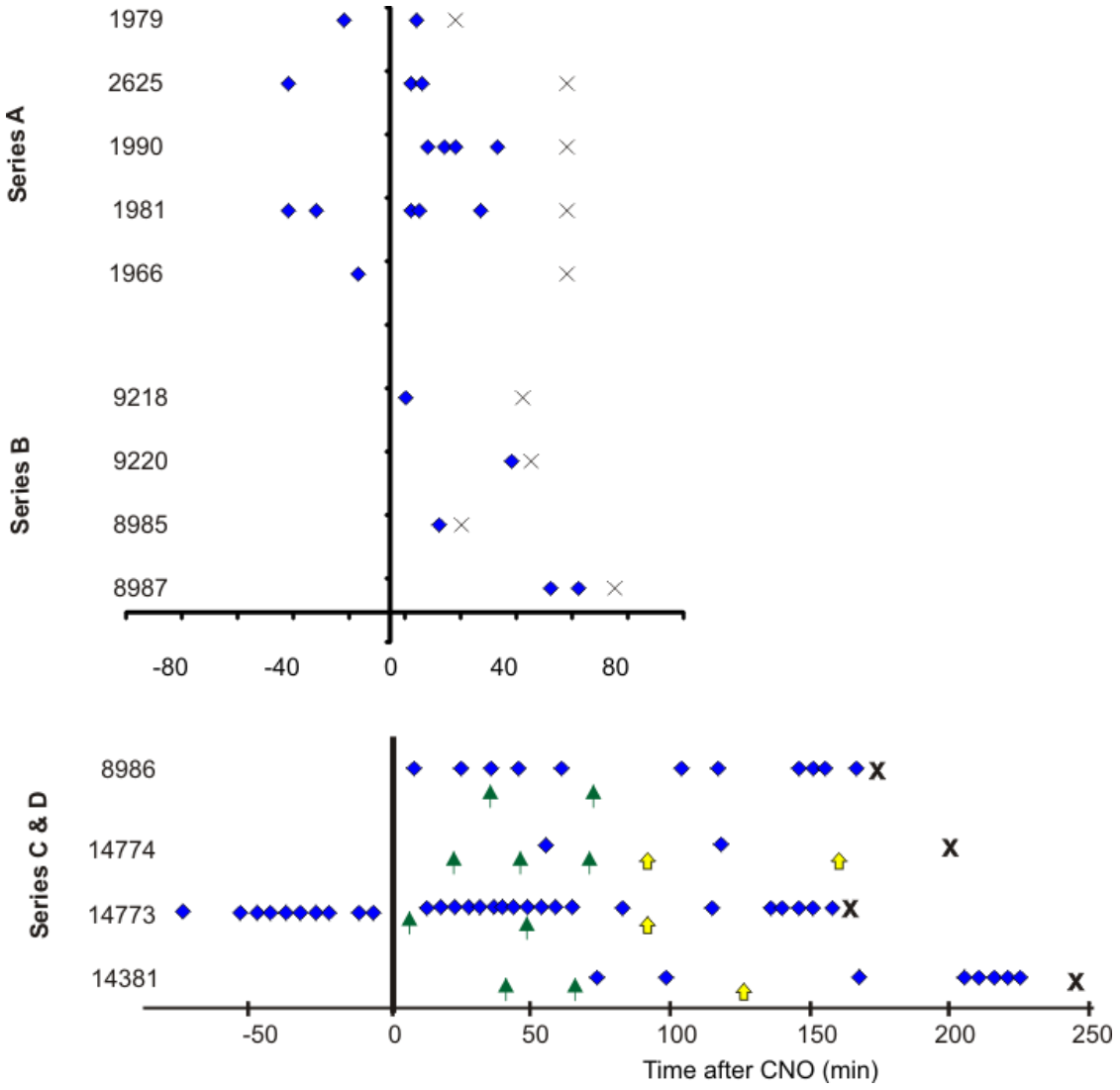

Figure 3.10 Quantitative summary of spontaneous activity
A schematic diagram to represent the instances of spontaneous activity. The X-axis indicates the time prior to and after the administration of CNO (zero point.) The negative numbers refer to the time before CNO administration while the positive time values indicate time after CNO administration up to the time of termination (X) of each experiment. The spontaneous activity is indicated as ♦ during a run. It is important to note that several bouts of spontaneous activity could occur during a 300s run, and the ♦ only represents whether any spontaneous activity occurred within these 300s. The spontaneous activity criteria was any type (tonic or phasic) ENG activity on one or more nerves lasting for at least 100 ms. Additional intracerebral CNO injections (50 nM, 500 nL) are indicated by a green arrow (→), and systemic injections of C21 (0.3 mg kg^{-1}) are indicated by a yellow arrow.

Overall, as shown in Fig 3.10 (and see spontaneous pre/post activity column of Table 3.1) there were two rats in which spontaneous activity did not occur either pre or post systemic CNO injections (both in series A). In two rats (one in series A and one in series B) spontaneous activity was present prior to systemic CNO injections but it was not evident after the injection. On the other hand, there were three animals manifesting spontaneous activity prior to systemic CNO injection with retaining them after the injection (as those in Fig. 3.8 B,D, and F). Moreover, the other seven animals did not exhibit spontaneous episodes prior to systemic CNO injection but developed spontaneous activity after CNO injections.

The combination of MLR and PPR electrical stimulation increased ENG burst duration based on the data from animals in Series A and B (see Fig 3.4) however this trend was not conserved after chemogenetic activation in combination with MLR stimulation. Fig 3.11 illustrates the average CP burst durations after administration of CNO normalized to pre-CNO bursts. In Series A, at 10-15 minutes after CNO, there was an increase in CP burst duration which was only observed in 2/10 animals of Series C and D after intracerebral CNO injections. Over time (20-50 minutes), however, the CP burst duration decreased in most animals of Series C and D (not statistically significant).

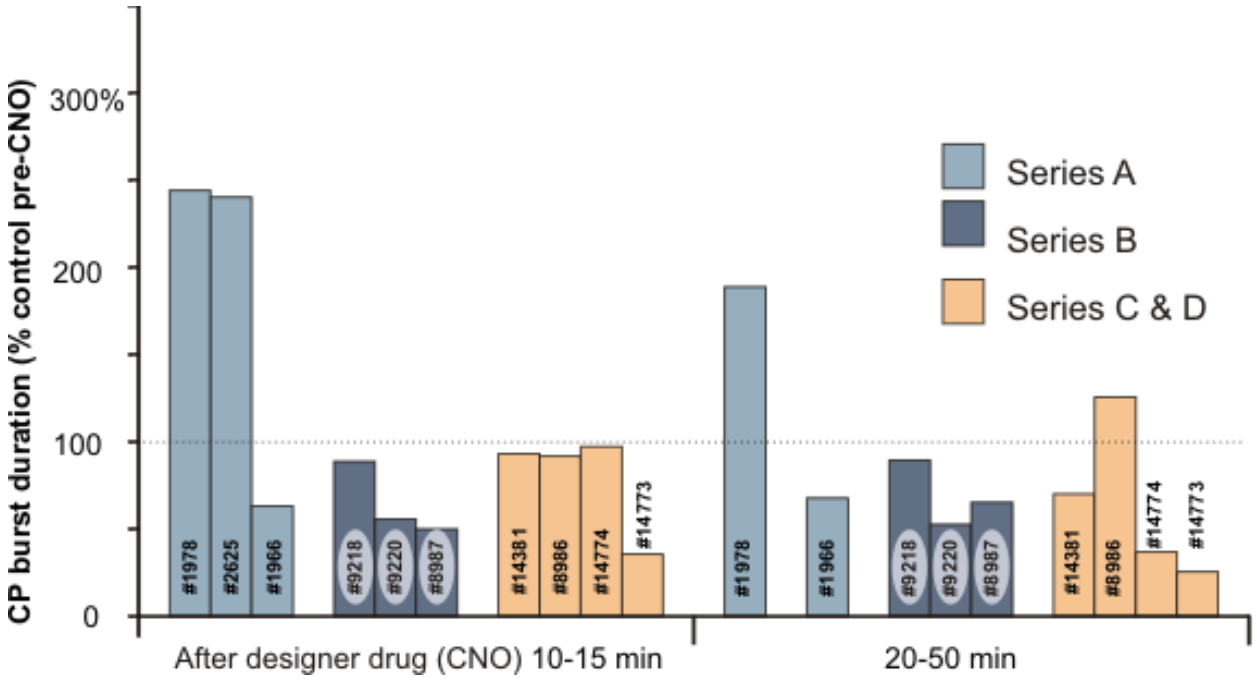

Figure 3.11 CP burst duration after CNO.
Average burst duration during 30 seconds of MLR stimulation (1 bout per rat) in animals from all series. The 100 percent CP burst duration represents the pre-CNO condition and the burst durations from CP. In all animals, 20-50 minutes after CNO are shown for all animals except #2625 in which ENG data was not available at 20 minutes after CNO (due to only tonic ENG output).

3.5. Selective chemogenetic stimulation of the PPR neurons via systemic CNO injections in awake, conscious rats during open field behavioural testing

The changes in the open field locomotor activity were evaluated on a subset of the animals in Series A and D. Those in Series A had a longer lasting open field test than animals in Series D but they were tested less frequently. The results from the open field test are summarized in Fig. 3.9 and they clearly convey some important aspects of open field testing. Firstly, the more time the animals spend in the open field box, the less they were willing to move. By the 15-20 min mark, even without any injection given, the animals had a tendency to rest within a corner (see Fig. 3.9A). In Series A, the number of crossed lines did not change significantly after CNO injections, albeit both the saline and the CNO injections reduced the animal's overall activity after 5 min and later following the injections when compared to no injections given. This can be seen when comparing the white bars vs. the blue and red bars Fig. 3.9.C).

There was a significant increase of the locomotor counts after CNO injections in Series D, as illustrated in Fig. 3.11D (star) with nearly a doubling of the locomotor counts (18-31 counts, $p=0.01$, paired t-test between the three saline sessions and the C21 session). The injection of C21 in both doses as well as CLOZ increased the locomotor counts, albeit there was not a significant difference ($p=0.1$, 0.06, 0.07 for C21 0.3 mg/kg, C21 1 mg/kg and CLOZ 0.3 mg/kg). The lack of the significant difference is likely due to the greater variability of the crossing counts in these versus the CNO conditions. The increase overall activity after the drug injections was mainly present in the first 5 minutes after the i.p. injections and later the counts were similar with saline and the other agents, at least within the 15 min that was monitored.

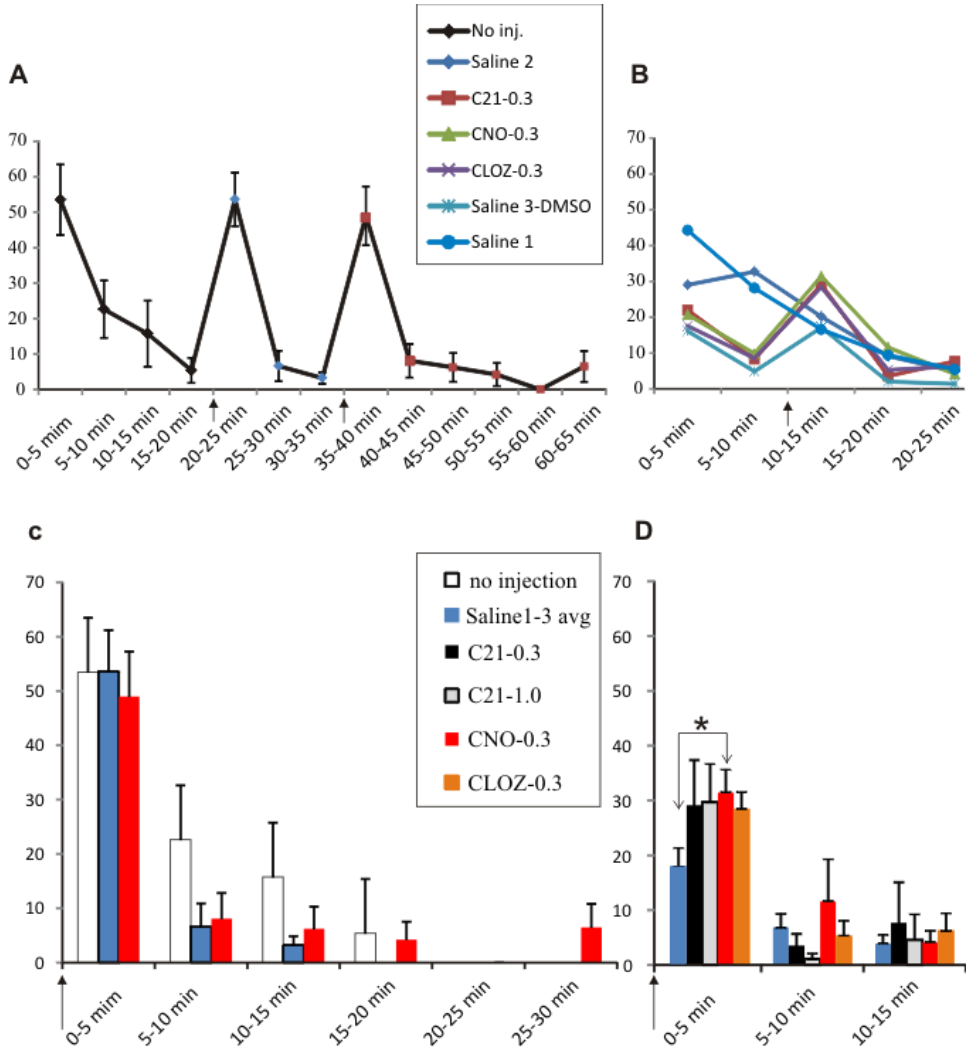

Figure 3.12 Summary of the locomotor activity during open field testing in adult, conscious rats.

A. Locomotor activity counted as the number of lines crossed in the open field box during the entire testing period (time zero on the X axis) for the 7 rats from Series A. The black arrows indicate the time of i.p. injections, first saline (0.9%, 0.3 mL) or CNO (0.3 mg/kg, 0.3 mL). The error bars indicate ±SEM.

B. Locomotor activity counted as the number of lines crossed in the open field box during the entire testing period (time zero on the X axis) for the 7 rats from Series D. The black arrow indicates the time of i.p. injection that was a different agent on the different testing days: saline (0.9%, sterile or with DMSO 1:2 ratio), clozapine-N-oxide (CNO 0.3 mg/kg), compound 21 (C21, 0.3 mg/kg or 1 mg/kg or clozapine (CLOZ, 0.3 mg/kg). The error bars indicating ±SEM were not included here for clarity.

C. Comparison of the locomotor activity in the various time periods with respect the i.p. injection in Series A. The black arrow indicates the time of i.p. injection.

D. Comparison of the locomotor activity in the various time periods with respect the i.p. injection in Series D, after averaging the three saline/DMSO trials.

3.6. Verification of m-Cherry reporter protein

Brain tissue from all animals have been collected for verification of the presence of the reporter protein associated with the designer receptors (m-Cherry) and tissue from 19/24 rats have been processed to date. Brain tissue from 18/19 rats harbouring injected constructs have shown the presence of the m-Cherry reporter similar to the illustrations in figure 3.1C-E. The process of summarizing the location and the number of the m-Cherry positive cells with respect to the PPR region and the stimulation sites of MLR and PPR electrical activation is still in progress. The percentage of 5-HT positive m-Cherry labeled neurons is also being counted in each animal, in order to estimate serotonergic versus ectopic expression. The amount of m-Cherry positive cells seemed to be similar in the animals with the lowest and the highest AAV transfection days. Analysis was done to examine whether there was a relationship between transfection days and effects on flexor burst duration. There was no linear relationship between the number of days with injected AAV constructs in the brain and the percent increase of R.CP burst durations ($r=0.0005$).

Chapter 4. Discussion

4.1. Summary of results

The first objective, to demonstrate that electrical stimulation limited to the vicinity of the PPR neurons to facilitate midbrain-stimulation evoked locomotor activity was partially met. The electrical stimulation of the PPR in the adult rat was found to significantly facilitate the burst duration of flexor nerves (Fig. 3.5) and occasionally, induce or facilitate extensor hindlimb nerve activity as well (Fig. 3.1 and 3.3). Occasionally, conditions were identified in which electrical PPR stimulation without MLR stimulation elicited fictive locomotion, but this was not the case in the majority of the tested animals.

The second objective, to demonstrate that selective activation of PPR neurons by using chemogenetic (DREADD) technology can initiate locomotion and/or facilitate midbrain-evoked fictive locomotor activity was dependent on the success of the combined genetically modified rat and the DREADD technology. The reported experiments in this thesis have shown that feasibility of the serotonergic neurons to incorporate and express designer receptors coupled to rAAV constructs in the Tph2-iCre driver rat model is high, as the presence of the reporter protein, m-Cherry, was found in 94% (17/18 rat brains) analysed to date. These findings emphasize that the Tph2-iCre rat model can be used for Cre-dependent transfection of PPR, as well as other serotonergic neurons, by the excitatory DREADDs tested here. The chemogenetic stimulation of the putative PPR neurons resulted in effects that were not all feasible to examine in terms of statistical significance, however, there were several examples of facilitation on lumbar motoneuron output as well as alteration of flexor-extensor coupling.

Increase in the incidences of spontaneous locomotor activity over half of the tested animals (10/14) and a reduction in only 2/14 rats after systemic CNO administration suggests that not only midbrain stimulation-induced locomotor activity is increased by PPR neurons but also they have an ability to trigger sufficient activity in the lumbar central pattern generator networks that is sufficient for evoking locomotion.

4.2. Interpreting the effects of electrical PPR stimulation in adult rats

The findings that PPR stimulation facilitates fictive motor output support the previous work done in the neonatal rat (Liu and Jordan 2005). Although, the electrical stimulation is not selective to the serotonergic neurons, we have used relatively low stimulus currents, 30-60 µA, in the adult rat experiments. These current intensities relate to a brain regions that are about 300 – 600 µm in diameter from the tip of the stimulating electrode as described in measurements obtained during adult cat spinal cord stimulations with similar type of electrodes (Gustafsson and Jankowska 1976). This suggests that the activation of neurons within 600 µm in the PPR region is conserved from neonatal to adult rats in terms of being able to facilitate the lumbar motor output, although, the role of the 5-HT neurons in terms of their specific effects on afferent input versus CPG neurons may change with development. The complete analysis of the location sites where the PPR electrodes (as well as the MLR electrodes) were positioned will allow more conclusive statements when interpreting the results from the decerebrate experiments.

The common observation, as in Fig. 3.4, indicating that PPR stimulation (when added to the ongoing MLR stimulation) increases the amplitude and the frequency of the rhythmic bursting activity of the hindlimb nerves supports that PPR stimulation does have a general facilitatory effect on motor output. The more specific role of PPR cells that was identified in

terms of their effects on “locomotor-like” hindlimb ENG profiles was the significantly increased burst durations in flexors (Fig. 3.5).

4.3. Interpreting the effects of chemogenetic PPR stimulation in adult rats

This genetic rat model was expected to allow that the hM3DGq designer receptors trigger neural firing after systemic CNO application, with the designer drug selectively binding at the designer receptors. Effects on the fictive locomotor output were difficult to quantify however there is evidence of facilitation early after CNO administration. This can be seen when comparing the ENG activity profiles before CNO injections in the same rats. Comparing Figures 3.1 to 3.6A, 3.3 to 3.6C and 3.4 to 3.6E with ENG activity from the same rats, before and after CNO application, respectively, shows that longer lasting rhythmic activity was often evident after CNO injections. At later time points after the systemic CNO application, electrical stimulation induced ENG activity exhibited deteriorating rhythmic activity (as in Fig 3.6 B, D, F). This deterioration was not always associated with the declining vital indicators of the animal’s health. This conserved effect may be due to the conversion of CNO to clozapine, which may in turn bind to multiple endogenous receptors (see later in Discussion and Table 4.1).

When assessing flexor and extensor coupling (Figure 3.7) the lack of changes in the r-values suggests that CNO application did not simply randomized the bursting of the two nerves, but it induced a shift that brought about a synchronous firing of flexor and extensor motoneurons. The increased burst durations in flexors after electrical PPR stimulation (Figure 3.5) contradict the examples when after CNO injections, very fast rhythmic activity developed. The fast rhythmic activity, as in Fig. 3.8, seems more like the fictive scratch pattern described in

decerebrate cats (Baev 1981). Cycles around 100-150 ms are closer to that described for scratching cycles in cats. However, fictive scratch has not been previously described in decerebrate rats.

The results obtained using chemogenetic stimulation with CNO, however, were difficult to interpret. The reasons for the difficulties were two-fold: 1) problems with the designer receptor expression and 2) ambiguity with CNO affecting the target ligands.

Initially, it was observed that the viral vectors obtained from UNC Vector core (used in Series A), were not only present in 5-HT neurons. In this series, it was found that in several brain sections from all rats that many neurons located near the injection site had the reporter protein of the DREADD construct but those cells did not show the presence of the marker for 5-HT. Currently, quantification of the percentage of the 5-HT positive neurons within all those cells expressing the m-Cherry reporter is in progress, but the preliminary inspections suggest that the percentage of transfected serotonergic neurons in series A is less than in series B and C. In series B and C, a viral vector construct was obtained from Addgene and it appears that m-Cherry was more specific to 5-HT neurons.

The reason for non-serotonergic neurons expressing the reporter protein could have been 1) transynaptic transfection of other cells by the AAVs and/or 2) non-specific (i.e. Cre-independent) translation of the constructs. Albeit there may be sufficient designer receptor in as low as 3, 7 or 14 days after the injections (Rothermel et al. 2013) these experiments examined much longer recovery or transfection periods as there was no previously available data on the time required to achieve the levels of designer receptors at this specific site of the brain targeted within this Cre-model. By comparing the transfected cell numbers (counting is ongoing) in those

animals that survived considerably longer than the others, (i.e. 20 days versus the 105 days survival animals, see Table 3.1) it will be determined whether there is a significant difference in the number of transfected cells due to recovery period.

In order to prevent the problem of non-specific (i.e. Cre-independent) translation of the constructs, the orientation of the cassette could have been validated using two or more primer pairs prior to the stereotaxic injections and animal experiments. In order to test that if the viral DNA is in the DIO orientation, ssDNA could be extracted from purified viruses. The polymerase chain reaction (PCR) products could be analysed by gel electrophoresis to ensure the correct banding pattern and sizers of the incorporated constructs. By using primers within and outside the loxP flanked regions, the presence of each functional DNA element would be identified. In the future, the quality of the vectors obtained will be examined by using this PCR-based method.

Another issue encountered during these experiments involved issues with the designer drug. Recent literature (i.e. Gomez et al. 2017) suggests that CNO does not cross the BBB and that the conversion of CNO to clozapine is occurring *in vivo*, at a high rate in mice and rats. It is most likely that clozapine is the actuator for the DREADDs.

4.4. Back metabolism and BBB penetrance of CNO

The designer drug, CNO, is the most commonly used ligand for the hM-DREADDs, with over 800 publications citing its use (English and Roth 2015). CNO has been advertised as an inert ligand (Armbruster et al. 2007) which is “CNS penetrant” (Ray et al. 2011; Bender, Holschbach, and Stöcklin 1994) and not subject to metabolic transformation in rodents (Chen et al. 2015). The parent compound clozapine, which is a commonly used antipsychotic agent, has two major metabolites, CNO and N-Desmethylclozapine (Schaber et al. 2002). It is already

known that CNO has the potential to back metabolize into both of these compounds in humans and guinea pigs (Jann et al. 1994; Chang et al. 1998). According to Alexander and colleagues (2009), CNO was selected as the synthetic ligand because "(i) its parent compound, clozapine, has high affinity to M3 receptors and therefore…few mutations would be required to permit CNO to be a potent agonist; (ii) CNO is highly bioavailable in rodents and humans; and (iii) importantly, CNO is a pharmacologically inert molecule lacking appreciable affinity for receptors" (Alexander et al. 2009). The potential for back metabolism in non-human primates has already limited DREADD application within these animals (Raper et al. 2017). Although some studies support the notion that CNO does not back metabolize in rodents (Jann et al. 1994), recent evidence has challenged these views. At higher doses of CNO (5 mg kg^{-1}), Maclaren and colleagues reported behavioural changes in Long-Evans rats lacking hM-DREADD receptors (MacLaren et al. 2016). Furthermore, they report that clozapine was detected in plasma at all time points with a maximum concentration at 30 minutes, approximately at $1/10^{th}$ the level of CNO at the same time point. They argue that their results coincide with early reports from a paper validating the DREADD technology (Guettier et al. 2009) which stated that the values of clozapine were not significant but nonetheless, appear to have a similar ratio of $1/10^{th}$ of the CNO (1 mg kg^{-1}) at the 30 minute time point. However, although Maclaren and colleagues reported behavioural effects at the commonly used doses (1-5 mg kg^{-1}) they were not able to replicate their results across all behavioural assays in their wild type control rats. Their initial finding showed minimal effect at 1 mg kg^{-1} CNO. Further replicates up to 2 mg kg^{-1} in the same paper fail to repeat effects even at higher doses (MacLaren et al. 2016).

Within their *ex vivo* locust model of the blood brain barrier, Hellman and colleagues (2016) stated that CNO was less likely to permeate the blood brain barrier and only low

concentrations of CNO were detected in the brain. Although this could have been because of the discrepancy between the locust model and a mammal model, they further conclude that there is no compelling evidence within the literature that CNO, when given systemically, is permeable in mammals (Hellman et al. 2016). The often cited reference to support that CNO is BBB permeable (Bender et al. 1994) fails to discriminate between the brain uptake of CNO and the amount of CNO formed in the brain from clozapine. Another study in which clozapine that was injected intraperitoneally in rats had no detectable levels of CNO within the brain, whereas serum concentrations equalled approximately 13% of clozapine, indicating peripheral metabolism but unable to be transported across the BBB (Baldessarini et al. 1993).

It has been suspected that very little CNO is able to cross the BBB, and there are not many studies that support the fact that it does. Raper et al. 2017, after administering a 10 mg kg^{-1} dose in non-human primates saw only 89-120 nM concentration of CNO in CSF (Raper et al. 2017). This dose may be at the lower end of an effective concentration range to activate hM-DREADDs after viral transfection. They suspected that CNO metabolites could be responsible for hM-DREADDs activation. Coupled to the fact that clozapine distributes to the CNS to a greater extent than CNO, it is possible that activation of hM-DREADDs could be mediated by clozapine.

Reviewing the pertaining literature should not discount all DREADD related studies but interpretation of the results requires consideration of metabolically derived clozapine. For example, the drastic response in body temperature after CNO administration (10 mg kg^{-1}) from the Dymecki lab (Ray et al. 2011) in DREADD mice could actually be symptoms of serotonin syndrome (SS) mediated by clozapine binding to 5-HT_{2A} receptors. It is well established that decrease in body temperature in mice is a symptom of SS (Haberzettl et al. 2013) and

consequently both activation of DREADDs in 5-HT neurons and non-specific binding of clozapine to 5-HT receptors may have contributed to 5-HT overdose.

In addition, previous studies have indicated that non-DREADD expressing cells show changes in activity after CNO administration. Chang and colleagues (2015), during recordings of ventral pallidal neurons in a behaving animal, noted a proportion of neurons not containing DREADDs responding to CNO application (Chang et al. 2015). They hypothesized that these cells may have been modulated through DREADD containing cells making contacts on non-DREADD neurons. However, it is a possibility that this noted effect may have been from clozapine.

Another recent publication has reported that 1) CNO may not cross the BBB and 2) the DREADD mediated effects are through clozapine which is highly CNS penetrant (Gomez et al. 2017). They suggest that "a combination of CNO conversion to clozapine, high clozapine brain permeability and high-affinity clozapine binding accounts for DREADD activation". By using radiolabelled CNO and clozapine ([11-Carbon] and [3-Hydrogen]) they demonstrated that CNO has very low CNS penetrance while clozapine can readily cross the BBB. These reports confound a previous study of radiolabelled CNO ([11C]-CNO) which reported the rapid entry of [11C]-CNO into the brain (Ji et al. 2016). It is possible that a major radio-metabolite of [11C]CNO could be [11C]Clozapine (Lin et al. 1996). However, using a dose that was 200 times less than previous reports (Ji et al. 2016) Gomez and colleagues report that no [11C]CNO signal was found (Gomez et al. 2017).

The evidence cited of CNO retro-conversion to clozapine is a very minimal amount in rodents (Guettier et al. 2009) but even this small amount is sufficient to activate DREADDs.

Even after a 1.5 µg kg^{-1} dose, clozapine shows a selective occupancy at hM4di and behavioural effects were observed at doses as low as 10 µg kg^{-1} (Gomez et al. 2017). With this very low, subthreshold concentration it appears that DREADDs are more sensitive to clozapine versus endogenous receptors, as there was very little evidence of non-specific binding of clozapine in other locations (Gomez et al. 2017). In addition, many labs using CNO as a control in wild type animals did not observe behavioural effects, indicating that the clozapine produced from CNO is not enough to induce significant behavioural changes. This has been countered by the results reported in the Series C from the above experiments. This is a very important observation because the majority of the published papers do not use clozapine as control. Further research will implement clozapine into the fictive locomotor experiments in order to strengthen this argument.

Clozapine has the potential to activate many other receptors other than the chemogenetic receptor. Below the table indicates the major serotonergic and other locomotor related receptors that could be identified with a *Ki* value of less than 520 based on the PDSP *Ki* database (Roth et al. 2000) Science Netwatch, {28 January 2000; 287 (5453)}. *Ki* is competition binding affinity constant that is a measure of how efficiently various ligands bind to a receptor. A lower *Ki* value indicates a higher binding efficiency.

5-HT receptors	Clozapine Ki	Other than 5-HT receptors	Clozapine Ki
5-HT2A	5.35	H1	1.13
5-HT2B	8.37	α1A	1.62
5-HT2C	9.44	α2C	6
5-HT6	13.49	M1	6.17
5-HT7	17.95	α1B	7
5-HT1A	123.7	M4	15.33
5-HT3	241	M5	15.5
5-HT1B	519	M3	19.25
		D4	26.36
		α2B	26.5
		M2	36.67
		α2A	37
		H2	153
		D2	157
		D5	255.33
		D1	266.25
		D3	269.08

Table 4.1 Affinity (Ki in uM) of clozapine on 5-HT and non-5-HT receptors
Competition binding affinity constants (K_i) for clozapine for certain receptors. Data obtained from PDSP Ki database (Roth et al. 2000) Science Netwatch, {28 January 2000; 287 (5453)}.

In DREADD related studies, the suggestion by Gomez et al. is to use clozapine as the actuator, as low doses are less likely to produce off target effects. However, researchers working with serotonergic and/or locomotor systems cannot benefit from this advice. Clozapine for locomotor suppression in rodents is widely acknowledged. Clozapine is known to affect receptors such as 5-HT_{1A}, 5-HT_{2A}, 5-HT_{2C} and 5-HT_7 (Meltzer 1999; Batool et al. 2010) which are important for the generation of locomotion (Hochman et al. 2001). In cats, using clozapine abolishes locomotion evoked by brainstem stimulation, analogous to the effect of clozapine in the in vitro neonatal rat (Liu and Jordan 2005; Schmidt and Jordan 2000). In adult rats, clozapine can decrease motor activity in a dose dependent manner (Batool et al. 2010).

One method to bypass the problem of CNS penetrance is by using intracerebral injections of CNO. As reported above, the effects on fictive locomotion with intracerebral injections of CNO were similar to those with systemic injections. Previous authors have used intracerebral injections (Mahler et al. 2014; Stachniak et al. 2014) but the disadvantage of this method is that it is invasive. As a control for future experiments, systemic and local injections of clozapine at minimal doses should also be used to determine what effect it may have on locomotion. It is important to note that clozapine has effects on dopamine, muscarinic and adrenergic receptors as well, therefore clozapine controls are important in the majority of studies utilizing hM-DREADDs in the future.

Another alternative approach is to use C21 which is an analog of CNO and a highly potent agonist for hM3Dq. However, effects of C21 has little data describing the biological activity (Chen et al. 2015). In that case, it is still unknown whether it is BBB penetrant. In addition, C21 is also a derivative of clozapine and could potentially metabolize into clozapine. Currently, there is no published evidence for metabolism of C21. However the data reported above shows the cessation of tonic and/or rhythmic brain stimulation induced fictive motor activity after C21 injections just like after CNO application. This could implicate that metabolites of C21 are present. For example, if C21 is also metabolized to clozapine that could be the reason for the observed effect.

4.5. Interpreting the behavioural effects

In Series A, there was a large difference between all the animals' locomotor capabilities even when comparing non-injected to saline injected sessions. In Series A, the animals were followed for a much longer time period within the open field box but the general trend was that

locomotion decreased with more time spent in the box. In the Series A, there were no significant changes after CNO administration on the overall locomotor activity.

After analyzing the results from Series A, it was determined further experiments with less open field time during trials would be more appropriate to determine the effects of specific activation of DREADDs on voluntary locomotion. In addition, new information about the potential for CNO to back metabolize into clozapine was available. It needed to be determined if larger doses of clozapine could affect locomotor counts. Interestingly, there were no significant differences in locomotor counts. Overall, there was a significant difference between saline injection and CNO (0.3 mg kg^{-1}) injection in the first five minutes. Similar locomotor counts were seen with C21 (low and high doses) and clozapine, which further imply the possibility of common metabolites.

4.6. Future improvements and considerations

In viral delivery models, it is very unlikely to achieve 100% penetrance even with very effective vectors. Using the common AAV8 vectors, it is estimated that approximately 2/3 of neurons will express the DREADD receptors (Smith et al. 2016). In addition, virally mediated transfection needs approximately 2-3 weeks for expression. Using transgenic rodents harbouring genetically altered neurons from birth circumvents the initial surgery required for intracranial delivery of viral constructs, as well a greater proportion of neurons within the area of interest would express DREADDs. The selective activation of the neurons within the target area would be the challenge, but for example, the intracranial injections of CNO used above would also make such experiments feasible in decerebrate, fictive locomotor preparations.

Spike frequency adaption (or accommodation) generally occurs when neurons show a plateauing in firing frequency after an initial increase. Repeated stimulation of DREADDs with any actuator can induce adaptation in theory. No in vivo studies have assessed how hM3DGq receptor activation influences accommodation. If the serotonergic neurons with DREADDs accommodate, their downstream targets in the spinal cord may also fail to show increased output. This could be underlying the cessation of ENG activity that we commonly observed after CNO application. Extracellular recordings from the serotonergic neurons would be necessary to address spike frequency adaption in response to CNO or other actuators of the DREADDs.

Further work is planned to transfect neurons with a combination of optogenetic constructs along with DREADDs to evaluate time locked effects of PPR stimulation in hindlimb ENGs. This approach could further validate that serotonergic neurons have significant actions on lumbar motoneurons during locomotion without the confounding factors related to CNO and its metabolites.

Another series of experiments validating serotonergic contributions to locomotion could be the loss of function studies. There are DREADDs that can induce inhibition of serotonergic neurons. If neuron inhibition is desired, the Gi-coupled DREADD using the kappa-opioid receptor as a template (KORD) may be a better alternative. This DREADD is activated by the inert ligand salvinorin B (Vardy et al. 2015).

4.7. Conclusion

Overall, the effects of electrical and chemogenetic stimulation on PPR 5-HT neurons was evaluated. While using combined electrical stimulation of the MLR and PPR, it was observed that average burst duration in flexor nerves increased (174±98%). When using systemic injections of CNO, no conclusions have been made as the potential of CNO back metabolizing into clozapine may have confounded these results. In the open field locomotor tests, there was an observed an initial increase in locomotion within five minutes and the increase was observed among all drugs tested. C21, the new DREADD agonist, when tested at lower dosages, seemed to maintain a higher level of locomotion compared to the other trials with other drugs. It is suspected that lower doses of C21 have less potential for back-metabolism into clozapine. The overall incidences of spontaneous activity in the decerebrate preparations after CNO administration were greater than before CNO. Using local intracerebral injections of CNO was more effective then systemic application of this designer drug albeit there were not enough experiments to achieve statistical significance. Further efforts will be directed towards testing the effects of back metabolism and collateral activation of other receptors. Further research will compare the use of optogenetic and chemogenetic constructs within the PPR to establish the importance of this region for locomotion in adult rats.

References

Abbinanti, Matthew D, Guisheng Zhong, and Ronald M Harris-Warrick. 2012. "Postnatal Emergence of Serotonin-Induced Plateau Potentials in Commissural Interneurons of the Mouse Spinal Cord." *Journal of Neurophysiology* 108 (8): 2191–2202. doi:10.1152/jn.00336.2012.

Alexander, Georgia M., Sarah C. Rogan, Atheir I. Abbas, Blaine N. Armbruster, Ying Pei, Allen John A., Randal J. Nonneman, et al. 2009. "Remote Control of Neuronal Activity in Transgenic Mice Expressing Evolved G Protein-Coupled Receptors." *Neuron* 63 (1): 27–39. doi:10.1016/j.neuron.2009.06.014.

Armbruster, Blaine N, Xiang Li, Mark H Pausch, Stefan Herlitze, and Bryan L Roth. 2007. "Evolving the Lock to Fit the Key to Create a Family of G Protein-Coupled Receptors Potently Activated by an Inert Ligand." *Proceedings of the National Academy of Sciences of the United States of America* 104 (12): 5163–68. doi:10.1073/pnas.0700293104.

Armstrong, D M. 1986. "Supraspinal Contributions to the Initiation and Control of Locomotion in the Cat." *Progress in Neurobiology* 26 (4): 273–361. http://www.ncbi.nlm.nih.gov/pubmed/3526411.

Baev, K. V. 1981. "The Central Program of Activation of Hind-Limb Muscles during Scratching in Cats." *Neurophysiology* 13 (1): 38–44. doi:10.1007/BF01073005.

Baldessarini, R J, F Centorrino, J G Flood, S A Volpicelli, D Huston-Lyons, and B M Cohen. 1993. "Tissue Concentrations of Clozapine and Its Metabolites in the Rat." *Neuropsychopharmacology : Official Publication of the American College of Neuropsychopharmacology* 9 (2): 117–24. doi:10.1038/npp.1993.50.

Barnes, Nicholas M., and Trevor Sharp. 1999. "A Review of Central 5-HT Receptors and Their Function." *Neuropharmacology* 38 (8): 1083–1152. doi:10.1016/S0028-3908(99)00010-6.

Batool, Farhat, Ambreen Hasnat, Muhammad Haleem, and Darakhshan Haleem. 2010. "Dose-Related Effects of Clozapine and Risperidone on the Pattern of Brain Regional Serotonin and Dopamine Metabolism and on Tests Related to Extrapyramidal Functions in Rats." *Acta Pharmaceutica* 60 (2): 129–40. doi:10.2478/v1007-010-0014-y.

Bender, D, M Holschbach, and G Stöcklin. 1994. "Synthesis of N.c.a. Carbon-11 Labelled Clozapine and Its Major Metabolite Clozapine-N-Oxide and Comparison of Their Biodistribution in Mice." *Nuclear Medicine and Biology* 21 (7): 921–25. http://www.ncbi.nlm.nih.gov/pubmed/9234345.

Bowker, R.M., K.N. Westlund, and J.D. Coulter. 1981. "Origins of Serotonergic Projections to the Spinal Cord in Rat: An Immunocytochemical-Retrograde Transport Study." *Brain Research* 226 (1–2): 187–99. doi:10.1016/0006-8993(81)91092-1.

Brust, Rachael D., Andrea E. Corcoran, George B. Richerson, Eugene Nattie, and Susan M. Dymecki. 2014. “Functional and Developmental Identification of a Molecular Subtype of Brain Serotonergic Neuron Specialized to Regulate Breathing Dynamics.” *Cell Reports* 9 (6): 2152–65. doi:10.1016/j.celrep.2014.11.027.

Cabaj, Anna M., Henryk Majczyński, Erika Couto, Phillip F. Gardiner, Katinka Stecina, Urszula Sławińska, and Larry M. Jordan. 2017. “Serotonin Controls Initiation of Locomotion and Afferent Modulation of Coordination via 5-HT $_7$ Receptors in Adult Rats.” *The Journal of Physiology* 595 (1): 301–20. doi:10.1113/JP272271.

Cazalets, J R, M Borde, and F Clarac. 1995. “Localization and Organization of the Central Pattern Generator for Hindlimb Locomotion in Newborn Rat.” *The Journal of Neuroscience : The Official Journal of the Society for Neuroscience* 15 (7 Pt 1): 4943–51. http://www.ncbi.nlm.nih.gov/pubmed/7623124.

Cazalets, J R, Y Sqalli-Houssaini, and F Clarac. 1992. “Activation of the Central Pattern Generators for Locomotion by Serotonin and Excitatory Amino Acids in Neonatal Rat.” *The Journal of Physiology* 455: 187–204. doi:10.1113/jphysiol.1992.sp019296.

Chang, Stephen E., Travis P. Todd, David J. Bucci, and Kyle S. Smith. 2015. “Chemogenetic Manipulation of Ventral Pallidal Neurons Impairs Acquisition of Sign-Tracking in Rats.” Edited by Rui Costa. *European Journal of Neuroscience* 42 (12): 3105–16. doi:10.1111/ejn.13103.

Chang, Wen Ho, Shih Ku Lin, Hsien Yuan Lane, Fu Chuan Wei, Wei Herng Hu, Y. W.Francis Lam, and Michael W. Jann. 1998. “Reversible Metabolism of Clozapine and Clozapine N-Oxide in Schizophrenic Patients.” *Progress in Neuro-Psychopharmacology and Biological Psychiatry* 22 (5): 723–39. doi:10.1016/S0278-5846(98)00035-9.

Charnay, Yves, and Lucienne Léger. 2010. “Brain Serotonergic Circuitries.” *Dialogues in Clinical Neuroscience* 12 (4): 471–87. http://www.pubmedcentral.nih.gov/articlerender.fcgi?artid=3181988&tool=pmcentrez&rendertype=abstract.

Chen, Xin, Hyunah Choo, Xi-Ping Huang, Xiaobao Yang, Orrin Stone, Bryan L. Roth, and Jian Jin. 2015. “The First Structure–Activity Relationship Studies for Designer Receptors Exclusively Activated by Designer Drugs.” *ACS Chemical Neuroscience* 6 (3): 476–84. doi:10.1021/cn500325v.

Cowley, K C, and B J Schmidt. 1997. “Regional Distribution of the Locomotor Pattern-Generating Network in the Neonatal Rat Spinal Cord.” *Journal of Neurophysiology* 77 (1): 247–59. http://www.ncbi.nlm.nih.gov/pubmed/9120567.

Dahlström, Annica, and Kjell Fuxe. 1964. “Evidence for the Existence of Monoamine-Containg Neurons in the Central Nervous System I. Demostrationof Monoamines in the Cellbodies of Brain Stem Neurons.” *Acta Physiologica Scandinavica. Supplementum* 18 (1): SUPPL

232:1-55. doi:10.1007/BF00160582.

Davidson, Beverly L, and Xandra O Breakefield. 2003. “Viral Vectors for Gene Delivery to the Nervous System.” *Nature Reviews. Neuroscience* 4 (5): 353–64. doi:10.1038/nrn1104.

Depuy, Seth D, Roy Kanbar, Melissa B Coates, Ruth L Stornetta, and Patrice G Guyenet. 2011. “Control of Breathing by Raphe Obscurus Serotonergic Neurons in Mice.” *The Journal of Neuroscience : The Official Journal of the Society for Neuroscience* 31 (6): 1981–90. doi:10.1523/JNEUROSCI.4639-10.2011.

Drew, T, R Dubuc, and S Rossignol. 1986. “Discharge Patterns of Reticulospinal and Other Reticular Neurons in Chronic, Unrestrained Cats Walking on a Treadmill.” *Journal of Neurophysiology* 55 (2): 375–401. http://www.ncbi.nlm.nih.gov/pubmed/3950696.

English, Justin G, and Bryan L Roth. 2015. “Chemogenetics-A Transformational and Translational Platform.” *JAMA Neurology* 72 (11): 1361–66. doi:10.1001/jamaneurol.2015.1921.

Gerin, C, and A Privat. 1998. “Direct Evidence for the Link between Monoaminergic Descending Pathways and Motor Activity: II. A Study with Microdialysis Probes Implanted in the Ventral Horn of the Spinal Cord.” *Brain Research* 794 (1): 169–73. http://www.ncbi.nlm.nih.gov/pubmed/9630613.

Gomez, Juan L, Jordi Bonaventura, Wojciech Lesniak, William B Mathews, Polina Sysa-shah, Lionel A Rodriguez, Randall J Ellis, et al. 2017. “Chemogenetics Revealed: Dreadd Occupancy and Activation Via Converted Clozapine.” *Science* 507 (August): 503–7. doi:10.1126/science.aan2475.

Grillner, S, and P Zangger. 1979. “On the Central Generation of Locomotion in the Low Spinal Cat.” *Experimental Brain Research* 34 (2): 241–61. http://www.ncbi.nlm.nih.gov/pubmed/421750.

Grillner, Sten, and Abdeljabbar El Manira. 2015. “The Intrinsic Operation of the Networks That Make Us Locomote.” *Current Opinion in Neurobiology* 31 (April): 244–49. doi:10.1016/j.conb.2015.01.003.

Guettier, Jean-Marc, Dinesh Gautam, Marco Scarselli, Inigo Ruiz de Azua, Jian Hua Li, Erica Rosemond, Xiaochao Ma, et al. 2009. “A Chemical-Genetic Approach to Study G Protein Regulation of Beta Cell Function in Vivo.” *Proceedings of the National Academy of Sciences of the United States of America* 106 (45): 19197–202. doi:10.1073/pnas.0906593106.

Gustafsson, B, and E Jankowska. 1976. “Direct and Indirect Activation of Nerve Cells by Electrical Pulses Applied Extracellularly.” *The Journal of Physiology* 258 (1): 33–61. http://www.ncbi.nlm.nih.gov/pubmed/940071.

Haberzettl, Robert, Bettina Bert, Heidrun Fink, and Meredith A Fox. 2013. “Animal Models of the Serotonin Syndrome: A Systematic Review.” *Behavioural Brain Research* 256 (November): 328–45. doi:10.1016/j.bbr.2013.08.045.

Helke, C.J., K.B. Thor, and C.A. Sasek. 1989. “Chapter 2 Chemical Neuroanatomy of the Parapyramidal Region of the Ventral Medulla in the Rat.” In , 17–28. doi:10.1016/S0079-6123(08)61997-4.

Hellman, Karin, Peter Aadal Nielsen, Fredrik Ek, and Roger Olsson. 2016. “An Ex Vivo Model for Evaluating Blood-Brain Barrier Permeability, Efflux, and Drug Metabolism.” *ACS Chemical Neuroscience* 7 (5): 668–80. doi:10.1021/acschemneuro.6b00024.

Hennessy, Morgan L., Andrea E. Corcoran, Rachael D. Brust, YoonJeung Chang, Eugene E. Nattie, and Susan M. Dymecki. 2017. “Activity of *Tachykinin1* -Expressing *Pet1* Raphe Neurons Modulates the Respiratory Chemoreflex.” *The Journal of Neuroscience* 37 (7): 1807–19. doi:10.1523/JNEUROSCI.2316-16.2016.

Hochman, Shawn, Sandra Garraway, David Machacek, and Barbara Shay. 2001. “5-HT Receptors and the Neuromodulatory Control of Spinal Cord Function.” In , 47–87. doi:10.1201/9781420042641.ch3.

Holtman, J R, L J Marion, and D F Speck. 1990. “Origin of Serotonin-Containing Projections to the Ventral Respiratory Group in the Rat.” *Neuroscience* 37 (2): 541–52. http://www.ncbi.nlm.nih.gov/pubmed/2133358.

Husch, Andreas, Shelby B Dietz, Diana N Hong, and Ronald M Harris-Warrick. 2015. “Adult Spinal V2a Interneurons Show Increased Excitability and Serotonin-Dependent Bistability.” *Journal of Neurophysiology* 113 (4): 1124–34. doi:10.1152/jn.00741.2014.

Jacobs, Barry L., and Casimir A. Fornal. 1993. “5-HT and Motor Control: A Hypothesis.” *Trends in Neurosciences* 16 (9): 346–52. doi:10.1016/0166-2236(93)90090-9.

Jacobs, Barry L, Francisco J Martín-Cora, and Casimir A Fornal. 2002. “Activity of Medullary Serotonergic Neurons in Freely Moving Animals.” *Brain Research. Brain Research Reviews* 40 (1–3): 45–52. http://www.ncbi.nlm.nih.gov/pubmed/12589905.

Jann, M W, Y W Lam, and W H Chang. 1994. “Rapid Formation of Clozapine in Guinea-Pigs and Man Following Clozapine-N-Oxide Administration.” *Archives Internationales de Pharmacodynamie et de Thérapie* 328 (2): 243–50. http://www.ncbi.nlm.nih.gov/pubmed/7710309.

Ji, Bin, Hiroyuki Kaneko, Takafumi Minamimoto, Haruhisa Inoue, Hiroki Takeuchi, Katsushi Kumata, Ming-Rong Zhang, et al. 2016. “Multimodal Imaging for DREADD-Expressing Neurons in Living Brain and Their Application to Implantation of iPSC-Derived Neural Progenitors.” *The Journal of Neuroscience : The Official Journal of the Society for Neuroscience* 36 (45): 11544–58. doi:10.1523/JNEUROSCI.1279-16.2016.

Jones, S. L., and A. R. Light. 1992. “Serotoninergic Medullary Raphespinal Projection to the Lumbar Spinal Cord in the Rat: A Retrograde Immunohistochemical Study.” *The Journal of Comparative Neurology* 322 (4): 599–610. doi:10.1002/cne.903220413.

Jordan, Larry M. 1986. “Initiation of Locomotion from the Mammalian Brainstem.” In *Neurobiology of Vertebrate Locomotion: Proceedings of an International Symposium Held at The Wenner-Gren Center, Stockholm, June 17th -- 19th, 1985*, edited by Sten Grillner, Paul S G Stein, Douglas G Stuart, Hans Forssberg, and Richard M Herman, 21–37. London: Palgrave Macmillan UK. doi:10.1007/978-1-349-09148-5_2.

Jordan, Larry M, Jun Liu, Peter B Hedlund, Turgay Akay, and Keir G Pearson. 2008. “Descending Command Systems for the Initiation of Locomotion in Mammals.” *Brain Research Reviews* 57 (1): 183–91. doi:10.1016/j.brainresrev.2007.07.019.

Kerman, Ilan A, Lynn W Enquist, Stanley J Watson, and Bill J Yates. 2003. “Brainstem Substrates of Sympatho-Motor Circuitry Identified Using Trans-Synaptic Tracing with Pseudorabies Virus Recombinants.” *The Journal of Neuroscience : The Official Journal of the Society for Neuroscience* 23 (11): 4657–66. doi:10.1016/0006-8993(84)90757-1.

Kiehn, Ole. 2016. “Decoding the Organization of Spinal Circuits That Control Locomotion.” *Nature Reviews Neuroscience* 17 (4): 224–38. doi:10.1038/nrn.2016.9.

Kjaerulff, O, and O Kiehn. 1996. “Distribution of Networks Generating and Coordinating Locomotor Activity in the Neonatal Rat Spinal Cord in Vitro: A Lesion Study.” *The Journal of Neuroscience : The Official Journal of the Society for Neuroscience* 16 (18): 5777–94. http://www.ncbi.nlm.nih.gov/pubmed/8795632.

Kjaerulff, Ole, and Ole Kiehn. 1996. “Distribution of Networks Generating and Coordinating Locomotor Activity in the Neonatal Rat Spinal Cord In Vitro : A Lesion Study” 16 (18): 5777–94.

Kudo, N, and T Yamada. 1987. “N-Methyl-D,L-Aspartate-Induced Locomotor Activity in a Spinal Cord-Hindlimb Muscles Preparation of the Newborn Rat Studied in Vitro.” *Neuroscience Letters* 75 (1): 43–48. http://www.ncbi.nlm.nih.gov/pubmed/3554010.

Lakke, E A. 1997. “The Projections to the Spinal Cord of the Rat during Development: A Timetable of Descent.” *Advances in Anatomy, Embryology, and Cell Biology* 135: I–XIV, 1-143. http://www.ncbi.nlm.nih.gov/pubmed/9257458.

Lee, A. Moses, Jennifer L. Hoy, Antonello Bonci, Linda Wilbrecht, Michael P. Stryker, and Cristopher M. Niell. 2014. “Identification of a Brainstem Circuit Regulating Visual Cortical State in Parallel with Locomotion.” *Neuron* 83 (2): 455–66. doi:10.1016/j.neuron.2014.06.031.

Lin, G, G McKay, and K K Midha. 1996. “Characterization of Metabolites of Clozapine N-Oxide in the Rat by Micro-Column High Performance Liquid Chromatography/mass

Spectrometry with Electrospray Interface." *Journal of Pharmaceutical and Biomedical Analysis* 14 (11): 1561–77. http://www.ncbi.nlm.nih.gov/pubmed/8877864.

Liu, J., T. Akay, P. B. Hedlund, K. G. Pearson, and L. M. Jordan. 2009. "Spinal 5-HT7 Receptors Are Critical for Alternating Activity During Locomotion: In Vitro Neonatal and In Vivo Adult Studies Using 5-HT7 Receptor Knockout Mice." *Journal of Neurophysiology* 102 (1): 337–48. doi:10.1152/jn.91239.2008.

Liu, Jun, and Larry M. Jordan. 2005. "Stimulation of the Parapyramidal Region of the Neonatal Rat Brain Stem Produces Locomotor-Like Activity Involving Spinal 5-HT7 and 5-HT2A Receptors." *Journal of Neurophysiology* 94 (2). http://jn.physiology.org.uml.idm.oclc.org/content/94/2/1392.

MacLaren, D. A. A., R. W. Browne, J. K. Shaw, S. Krishnan Radhakrishnan, P. Khare, R. A. Espana, and S. D. Clark. 2016. "Clozapine N-Oxide Administration Produces Behavioral Effects in Long-Evans Rats: Implications for Designing DREADD Experiments." *eNeuro* 3 (5). doi:10.1523/ENEURO.0219-16.2016.

Madriaga, M A, L C McPhee, T Chersa, K J Christie, and P J Whelan. 2004. "Modulation of Locomotor Activity by Multiple 5-HT and Dopaminergic Receptor Subtypes in the Neonatal Mouse Spinal Cord." *Journal of Neurophysiology* 92 (3): 1566–76. doi:10.1152/jn.01181.2003.

Mahler, Stephen V, Elena M Vazey, Jacob T Beckley, Colby R Keistler, Ellen M McGlinchey, Jennifer Kaufling, Steven P Wilson, Karl Deisseroth, John J Woodward, and Gary Aston-Jones. 2014. "Designer Receptors Show Role for Ventral Pallidum Input to Ventral Tegmental Area in Cocaine Seeking." *Nature Neuroscience* 17 (4): 577–85. doi:10.1038/nn.3664.

Marson, L., K.B. Platt, and K.E. McKenna. 1993. "Central Nervous System Innervation of the Penis as Revealed by the Transneuronal Transport of Pseudorabies Virus." *Neuroscience* 55 (1): 263–80. doi:10.1016/0306-4522(93)90471-Q.

Mason, Peggy. 2001. "Contributions of the Medullary Raphe and Ventromedial Reticular Region to Pain Modulation and Other Homeostatic Functions." *Annual Review of Neuroscience* 24: 737–77.

McCrea, David A, and Ilya A Rybak. 2008. "Organization of Mammalian Locomotor Rhythm and Pattern Generation." *Brain Research Reviews* 57 (1): 134–46. doi:10.1016/j.brainresrev.2007.08.006.

Meltzer, H. 1999. "The Role of Serotonin in Antipsychotic Drug Action." *Neuropsychopharmacology* 21 (2): 106S–115S. doi:10.1016/S0893-133X(99)00046-9.

Noga, Brian R., and I Opris. 2017. *The Physics of the Mind and Brain Disorders*. Edited by Ioan Opris and Manuel F. Casanova. Vol. 11. Springer Series in Cognitive and Neural Systems.

Cham: Springer International Publishing. doi:10.1007/978-3-319-29674-6.

Noga, Brian R., Francisco J. Sanchez, Luz M. Villamil, Christopher O'Toole, Stefan Kasicki, Maciej Olszewski, Anna M. Cabaj, Henryk Majczyński, Urszula Sławińska, and Larry M. Jordan. 2017. "LFP Oscillations in the Mesencephalic Locomotor Region during Voluntary Locomotion." *Frontiers in Neural Circuits* 11 (May): 1–17. doi:10.3389/fncir.2017.00034.

Noga, Brian R, Dawn M G Johnson, Mirta I Riesgo, and Alberto Pinzon. 2009. "Locomotor-Activated Neurons of the Cat. I. Serotonergic Innervation and Co-Localization of 5-HT7, 5-HT2A, and 5-HT1A Receptors in the Thoraco-Lumbar Spinal Cord." *J. Neurophysiol.* 102 (3): 1560–76. http://jn.physiology.org/cgi/reprint/102/3/1560.pdf.

Noga, Brian R, Dean J Kriellaars, Robert M Brownstone, and Larry M Jordan. 2003. "Mechanism for Activation of Locomotor Centers in the Spinal Cord by Stimulation of the Mesencephalic Locomotor Region." *Journal of Neurophysiology* 90 (3): 1464–78. doi:10.1152/jn.00034.2003.

Peterson, B W. 1979. "Reticulospinal Projections to Spinal Motor Nuclei." *Annual Review of Physiology* 41 (1): 127–40. doi:10.1146/annurev.ph.41.030179.001015.

Pierce, Kristen L., Richard T. Premont, and Robert J. Lefkowitz. 2002. "Signalling: Seven-Transmembrane Receptors." *Nature Reviews Molecular Cell Biology* 3 (9): 639–50. doi:10.1038/nrm908.

Rajaofetra, N., F. Sandillon, M. Geffard, and A. Privat. 1989. "Pre- and Post-Natal Ontogeny of Serotonergic Projections to the Rat Spinal Cord." *Journal of Neuroscience Research* 22 (3): 305–21. doi:10.1002/jnr.490220311.

Raper, Jessica, Ryan D. Morrison, J. Scott Daniels, Leonard Howell, Jocelyne Bachevalier, Thomas Wichmann, and Adriana Galvan. 2017. "Metabolism and Distribution of Clozapine-N-Oxide: Implications for Nonhuman Primate Chemogenetics." *ACS Chemical Neuroscience* 8 (7): 1570–76. doi:10.1021/acschemneuro.7b00079.

Ray, Russell S., Andrea E. Corcoran, Rachael D. Brust, Laura P. Soriano, Eugene E. Nattie, and Susan M. Dymecki. 2013. "Egr2-Neurons Control the Adult Respiratory Response to Hypercapnia." *Brain Research* 1511 (1): 115–25. doi:10.1016/j.brainres.2012.12.017.

Ray, Russell S, Andrea E Corcoran, Rachael D Brust, Jun Chul Kim, George B Richerson, Eugene Nattie, and Susan M Dymecki. 2011. "Impaired Respiratory and Body Temperature Control upon Acute Serotonergic Neuron Inhibition." *Science (New York, N.Y.)* 333 (6042): 637–42. doi:10.1126/science.1205295.

Ribotta, M G, J Provencher, D Feraboli-Lohnherr, S Rossignol, A Privat, and D Orsal. 2000. "Activation of Locomotion in Adult Chronic Spinal Rats Is Achieved by Transplantation of Embryonic Raphe Cells Reinnervating a Precise Lumbar Level." *The Journal of Neuroscience : The Official Journal of the Society for Neuroscience* 20 (13): 5144–52.

doi:20/13/5144 [pii].

Riddle, C. N., S. A. Edgley, and S. N. Baker. 2009. “Direct and Indirect Connections with Upper Limb Motoneurons from the Primate Reticulospinal Tract.” *Journal of Neuroscience* 29 (15): 4993–99. doi:10.1523/JNEUROSCI.3720-08.2009.

Roseberry, Thomas K., A. Moses Lee, Arnaud L. Lalive, Linda Wilbrecht, Antonello Bonci, and Anatol C. Kreitzer. 2016. “Cell-Type-Specific Control of Brainstem Locomotor Circuits by Basal Ganglia.” *Cell* 164 (3). doi:10.1016/j.cell.2015.12.037.

Roth, Bryan L., Estelle Lopez, Shamil Patel, and Wesley K. Kroeze. 2000. “The Multiplicity of Serotonin Receptors: Uselessly Diverse Molecules or an Embarrassment of Riches?” *The Neuroscientist* 6 (4): 252–62. doi:10.1177/107385840000600408.

Rothermel, Markus, Daniela Brunert, Christine Zabawa, Marta Díaz-Quesada, and Matt Wachowiak. 2013. “Transgene Expression in Target-Defined Neuron Populations Mediated by Retrograde Infection with Adeno-Associated Viral Vectors.” *The Journal of Neuroscience : The Official Journal of the Society for Neuroscience* 33 (38): 15195–206. doi:10.1523/JNEUROSCI.1618-13.2013.

Ryczko, Dimitri, and Réjean Dubuc. 2013. “The Multifunctional Mesencephalic Locomotor Region.” *Current Pharmaceutical Design* 19 (24): 4448–70. http://www.ncbi.nlm.nih.gov/pubmed/23360276.

Ryczko, Dimitri, Swantje Grätsch, Laura Schläger, Avo Keuyalian, Zakaria Boukhatem, Claudia Garcia, François Auclair, Ansgar Büschges, and Réjean Dubuc. 2017. “Nigral Glutamatergic Neurons Control the Speed of Locomotion.” *The Journal of Neuroscience* 37 (40): 9759–70. doi:10.1523/JNEUROSCI.1810-17.2017.

Samulski, R. Jude, and Nicholas Muzyczka. 2014. “AAV-Mediated Gene Therapy for Research and Therapeutic Purposes.” *Annual Review of Virology* 1 (1): 427–51. doi:10.1146/annurev-virology-031413-085355.

Schaber, Stevens, Gaertner, Dietz, and Breyer-Pfaff. 2002. “Pharmacokinetics of Clozapine and Its Metabolites in Psychiatric Patients: Plasma Protein Binding and Renal Clearance.” *British Journal of Clinical Pharmacology* 46 (5): 453–59. doi:10.1046/j.1365-2125.1998.00822.x.

Schmidt, Brian J., and Larry M. Jordan. 2000. “The Role of Serotonin in Reflex Modulation and Locomotor Rhythm Production in the Mammalian Spinal Cord.” *Brain Research Bulletin* 53 (5): 689–710.

Shik, M. L., F. V. Severin, and G. N. Orlovsky. 1966. “Control of Walking and Running by Means of Electrical Stimulation of the Mid-Brain.” *Biophysics* 11: 756–65.

Shik, M L, and G N Orlovsky. 1976. “Neurophysiology of Locomotor Automatism.”

Physiological Reviews 56 (3): 465–501. http://www.ncbi.nlm.nih.gov/pubmed/778867.

Skagerberg, G, and A Björklund. 1985. “Topographic Principles in the Spinal Projections of Serotonergic and Non-Serotonergic Brainstem Neurons in the Rat.” *Neuroscience* 15 (2): 445–80. http://www.ncbi.nlm.nih.gov/pubmed/4022334.

Skinner, R D, and E Garcia-Rill. 1984. “The Mesencephalic Locomotor Region (MLR) in the Rat.” *Brain Research* 323 (2): 385–89. http://www.ncbi.nlm.nih.gov/pubmed/6525525.

Sławińska, Urszula, Krzysztof Miazga, Anna M. Cabaj, Anna N. Leszczyńska, Henryk Majczyński, James I. Nagy, and Larry M. Jordan. 2013. “Grafting of Fetal Brainstem 5-HT Neurons into the Sublesional Spinal Cord of Paraplegic Rats Restores Coordinated Hindlimb Locomotion.” *Experimental Neurology* 247 (September): 572–81. doi:10.1016/j.expneurol.2013.02.008.

Smith, J C, and J L Feldman. 1987. “In Vitro Brainstem-Spinal Cord Preparations for Study of Motor Systems for Mammalian Respiration and Locomotion.” *Journal of Neuroscience Methods* 21 (2–4): 321–33. http://www.ncbi.nlm.nih.gov/pubmed/2890797.

Smith, Kyle S., David J. Bucci, Bryan W. Luikart, and Stephen V. Mahler. 2016. “DREADDS: Use and Application in Behavioral Neuroscience.” *Behavioral Neuroscience* 130 (2): 137–55. doi:10.1037/bne0000135.

Stachniak, Tevye J., Anirvan Ghosh, and Scott M. Sternson. 2014. “Chemogenetic Synaptic Silencing of Neural Circuits Localizes a Hypothalamus→Midbrain Pathway for Feeding Behavior.” *Neuron* 82 (4): 797–808. doi:10.1016/j.neuron.2014.04.008.

Steinbusch, H W. 1981. “Distribution of Serotonin-Immunoreactivity in the Central Nervous System of the Rat-Cell Bodies and Terminals.” *Neuroscience* 6 (4): 557–618. http://www.ncbi.nlm.nih.gov/pubmed/7017455.

Stuart, Douglas G, and Hans Hultborn. 2008. “Thomas Graham Brown (1882--1965), Anders Lundberg (1920-), and the Neural Control of Stepping.” *Brain Research Reviews* 59 (1): 74–95. doi:10.1016/j.brainresrev.2008.06.001.

Takakusaki, Kaoru, Ryosuke Chiba, Tsukasa Nozu, and Toshikatsu Okumura. 2016. “Brainstem Control of Locomotion and Muscle Tone with Special Reference to the Role of the Mesopontine Tegmentum and Medullary Reticulospinal Systems.” *Journal of Neural Transmission* 123 (7): 695–729. doi:10.1007/s00702-015-1475-4.

Thankachan, S, P M Fuller, and J Lu. 2012. “Movement- and Behavioral State-Dependent Activity of Pontine Reticulospinal Neurons.” *Neuroscience* 221 (September): 125–39. doi:10.1016/j.neuroscience.2012.06.069.

Tyce, G. 1990. “Origin and Metabolism of Serotonin.” *Journal of Cardiovascular Pharmacology* 16: Suppl. (3): S1–7.

Urban, Daniel J., and Bryan L. Roth. 2015. “DREADDs (Designer Receptors Exclusively Activated by Designer Drugs): Chemogenetic Tools with Therapeutic Utility.” *Annual Review of Pharmacology and Toxicology* 55 (1): 399–417. doi:10.1146/annurev-pharmtox-010814-124803.

Urban, Daniel J, Hu Zhu, Catherine A Marcinkiewcz, Michael Michaelides, Hidehiro Oshibuchi, Darren Rhea, Dipendra K Aryal, et al. 2016. “Elucidation of The Behavioral Program and Neuronal Network Encoded by Dorsal Raphe Serotonergic Neurons.” *Neuropsychopharmacology* 41 (5): 1404–15. doi:10.1038/npp.2015.293.

Veasey, S C, C a Fornal, C W Metzler, and B L Jacobs. 1995. “Response of Serotonergic Caudal Raphe Neurons in Relation to Specific Motor Activities in Freely Moving Cats.” *The Journal of Neuroscience : The Official Journal of the Society for Neuroscience* 15 (7 Pt 2): 5346–59.

Waldrop, Tony G, Frederic L Eldridge, Gary a Iwamoto, and Jere H Mitchell. 2011. “Central Neural Control of Respiration and Circulation During Exercise.” *Comprehensive Physiology*, no. 109: 333–80. doi:10.1002/cphy.cp120109.

Weber, Tillmann, Kai Schönig, Björn Tews, and Dusan Bartsch. 2011. “Inducible Gene Manipulations in Brain Serotonergic Neurons of Transgenic Rats.” Edited by Ya-Ping Tang. *PLoS ONE* 6 (11): e28283. doi:10.1371/journal.pone.0028283.

Weston, Matthew C, Ruth L Stornetta, and Patrice G Guyenet. 2004. “Glutamatergic Neuronal Projections from the Marginal Layer of the Rostral Ventral Medulla to the Respiratory Centers in Rats.” *The Journal of Comparative Neurology* 473 (1): 73–85. doi:10.1002/cne.20076.

Whelan, Patrick J. 1996. “Control of Locomotion in the Decerebrate Cat.” *@ Pergamon Progress in Neurobiology* 49 (403): 481–515. doi:10.1016/0301-0082(96)00028-7.

Whissell, Paul D., Sarasa Tohyama, and Loren J. Martin. 2016. “The Use of DREADDs to Deconstruct Behavior.” *Frontiers in Genetics*. doi:10.3389/fgene.2016.00070.

Yang, H, P.-Q Yuan, L Wang, and Y Taché. 1999. “Activation of the Parapyramidal Region in the Ventral Medulla Stimulates Gastric Acid Secretion through Vagal Pathways in Rats.” *Neuroscience* 95 (3): 773–79. doi:10.1016/S0306-4522(99)00490-X.

Appendix A. DREADD PET Imaging Analysis

Author list/Role:

1. Katrina Armstrong – *MSc Student*, University of Manitoba. Participated in all experiments in the injections of constructs, monitoring of animals during and after the MR imaging, all behavioral experiments and assisted in the post-hoc processing of the brain tissue as well analysis of the imaging data.

2. Xiaoyu Chen – *Postdoctoral Fellow*, University of Manitoba. Participated in all experiments in the injections of constructs, monitoring of animals during and after the MR imaging, all behavioral experiments and primarily responsible for the post-hoc processing and immunohistochemistry of the brain tissue.

3. Bryan McIntosh – *Physicist*, Cubresa Inc. Analyzed results from PET/fMRI study using VivoQuant and SPM8. Prepared detailed report on results.

4. Erika Couto-Roldan – *Technician*, University of Manitoba. Assisted with anatomical reconstruction of the brain regions with neurons that were found positive for the reporter protein (m-Cherry).

5. Richard Buist – *Researcher,* University of Manitoba. Responsible for operation of the PET/fMRI machine.

6. Melanie Martin – *Researcher*, University of Winnipeg and University of Manitoba.

7. John Saunders – *Chief Science Officer*, Cubresa Inc.

8. Larry Jordan – *Professor*, University of Manitoba.

9. Katinka Stecina – *Assistant Professor*, University of Manitoba.

Previously, methods used to study whole-brain functional activity has included post-mortem analysis of markers such as c-fos. However, improvements in imaging technologies have allowed for more direct investigations of specific cell populations. These included in vivo blood oxygenation level-dependent measures (e.g. functional magnetic resonance imaging, fMRI) or glucose utilization (e.g. Positron Emission Tomography, PET). These are more direct measures of neural activity, but both have certain pitfalls. However, by combining these two imaging modalities, there is the potential to overcome some of the limitations of each method. Cubresa has recently developed a multimodal imaging tool that allows for combination of both PET/fMRI. They are currently testing the accuracy and utility of their in-bore PET insert for 7T MRI scanners. Recently, we have collaborated with this group as another method to detect neural activation in our DREADD containing cells of the PPR. It is hypothesized that after administration of the designer drug, CNO, there would be an increase in blood oxygenation and glucose utilization within this region.

For this collaboration, I received training in radioactive safety and became certified to administer i.p. Injections of 18F-FDG. My primary contributions within this collaboration included animal welfare, such as transporting the animals and monitoring vitals during the imaging sessions, as well as administering FDG and organizing imaging sessions with members of Cubresa. During this time I learned about image acquisition and pre-processing of data related to neuroimaging. During the generation of the results report (presented below), I was the primary contact for specifics relating to the experimental procedures (e.g. FDG dosages). I received a full copy of the raw data presented below and began practicing analysis of this data on specialized software. The results of the analyses were inconclusive, and some of the potential issues may have been from the functionality of the insert or the DREADD technology.

Previous groups have reported statistically significant differences using DREAMM (DREADD Assisted Multi-Modality imaging) (Urban et al. 2016). Future work will be done to reanalyze and improve the experimental protocol. Despite the reported issues of DREADDs above, the potential for clozapine to cross the BBB and activate DREADDs should have resulted in more significant differences between saline injected and CNO injected animals.

The report presented below has been prepared by **Bryan McIntosh (Cubresa)**

Introduction

In an attempt to develop imaging protocols for rats who have been treated with DREADD (Designer Receptor Exclusively Activated by Designer Drug) agents, a set of six five rats were imaged using both FDG PET and fMRI (attempted 6 animals but one was lost due to irreversible heart rate drop while in the scanner). Ideally, animals which have been injected with the designer drug CNO should see selective activation of neurons that were treated with an injection of a DREADD viral agent. The same animal should see much less activation in that part of the brain with an injection of a saline solution. This should cause an increase in signal in a normalized FDG-PET image in rats given CNO compared to rats injected with saline.

This report summarizes the statistical parametric mapping (SPM) results from the PET and fMRI data. SPM compares a set of images on a voxel-by-voxel basis to determine whether there is a statistically significant variation between data sets, and the magnitude of that difference above background noise.

Methods

Five rats that had been treated to express DREADD were imaged on August 23, August 24, August 29, and August 31 2016. Each rat imaging session was preceded by a simultaneous injection of 18F-FDG and either the CNO neuron-activating drug or a saline injection. One hour of PET imaging began nominally 15 minutes post-injection with a series of 15 minute long scans to track the uptake of tracer post-injection. CNO and saline imaging sessions were performed on different days to allow for complete clearance of the drug and tracer material. The schedule of animal imaging and injections is shown in the following table.

Table A1. Description of experimental schedule

Date	Rat #	Rat ID	Injection	Injected Radioactivity (MBq)
Aug. 23, 2016	1	1981-2R	Saline	23.24
	2	1979-R	CNO	25.13
	3	1989-R	CNO	27.40
Aug. 24, 2016	1	2624	CNO	21.45
	2	2625	CNO	23.70
Aug. 29, 2016	1	1979-R	Saline	26.20
	2	1989-R	Saline	26.90
Aug. 31, 2016	1	1981-2R	CNO	28.80
	2	2624	Saline	23.70
	3	2625	Saline	28.00

A structural T2 MRI scan was performed during the PET acquisition period to provide an anatomical co-reference. These images were acquired as 256 x 256 x 128 volumes (voxel size 0.20 x 0.20 x 0.39 mm3) that were resliced to 256x256x256 images within VivoQuant during viewing.

PET images were reconstructed using STIR's OSMAPOSL algorithm (25 iterations, 1 subset) with no scatter or attenuation correction applied to the data set. Each image was co-

registered with its corresponding MR scan and segmented manually using VivoQuant's 3D ROI tools so that only the brain volume of each PET and MR scan contained non-zero voxel values.

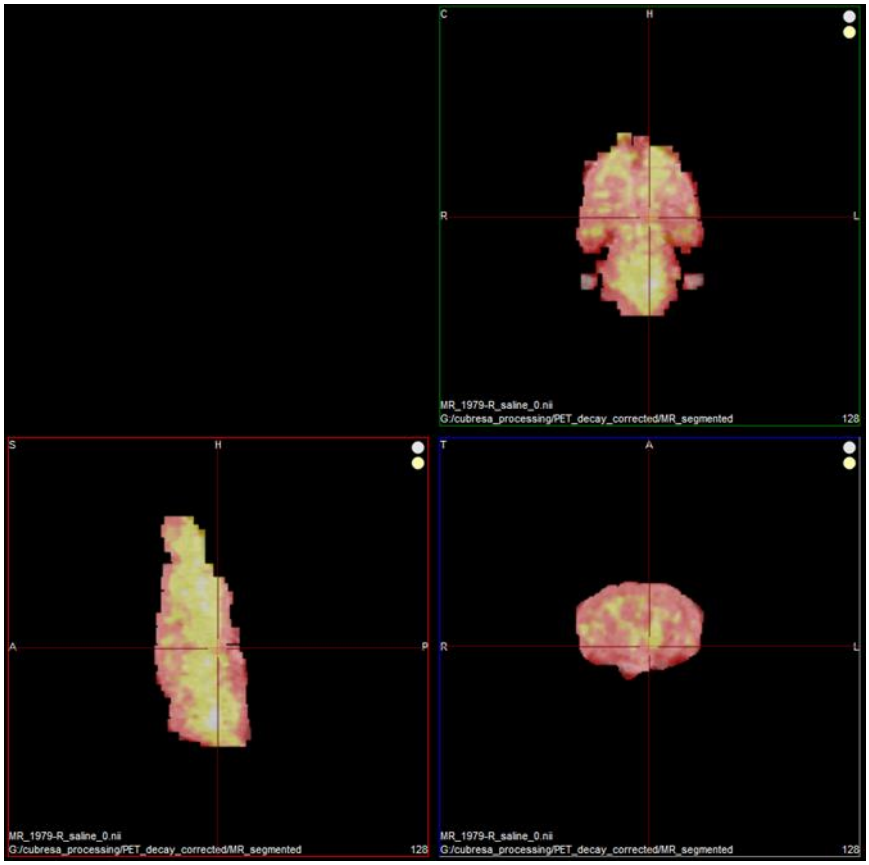

Figure A1: Co-registered, segmented PET and MR images from the 45 minute time point of rat 1979-R.

After segmentation, each animal's four PET scans were run through the automated co-registration routine in the Small Animal Imaging Toolkit (SAMIT) to ensure that each data set matched with the structural MR scan of the animal's CNO-injected scan. This ensured that the SPM analysis would be able to compare on a voxel-to-voxel basis between scans with CNO injected versus saline-injected scans. Each co-registered image was then loaded into MATLAB where all voxel values were normalized to the total number of counts in the brain. This step was performed to correct for differences in animal uptake between scan days as well as small differences in injected activity.

After pre-processing, a two-sample t-test was performed using SPM8. The PET scans corresponding to the saline scan were chosen as Group 1, and the CNO scans were placed in Group 2. The T2-weighted structural MR scan from the CNO trial was used as a spatial mask for the analysis to minimize chances of SPM seeing differences outside of the brain volume. Images were created with a significance threshold of $p < 0.05$, leading to maps of T values that express differences between the two data sets divided by the noise in the image.

fMRI data sets were acquired using a T2 RARE pulse sequence. 37 scans were performed during each imaging session concurrently with the PET acquisition. Each scan lasted for 98.56 seconds with a TE of 24.5 ms, TR of 1540 ms, and 2 averages. Scan data were binned into 128 x 128 x 5 images, with voxel sizes of 0.254 x 0.254 x 0.635 mm3.

This fMRI data was segmented using VivoQuant to remove voxels outside the brain region. fMRI data sets were analyzed using SPM8's fMRI First Level analysis. Each animal's two imaging sessions were compared to each other on a CNO/saline pairwise basis. The timing parameters were set to "scans" as the unit for the design and the interscan interval was set to 98.56 seconds. The canonical heart rate function was chosen during analysis, and images were normalized using SPM's Global Normalization set to "scaling."

Results – PET Data

These images consist of a greyscale T2 weighted structural MR scan of the rat's brain overlaid with a black-orange-red-yellow colourscale representing voxels where the PET data showed statistically greater uptake ($p < 0.05$) in the CNO imaging session versus the saline imaging session. T values corresponding to these voxels are written below each slice. Greater T

values correspond to stronger differences between the two imaging sessions at that voxel location.

Rat 1979-R

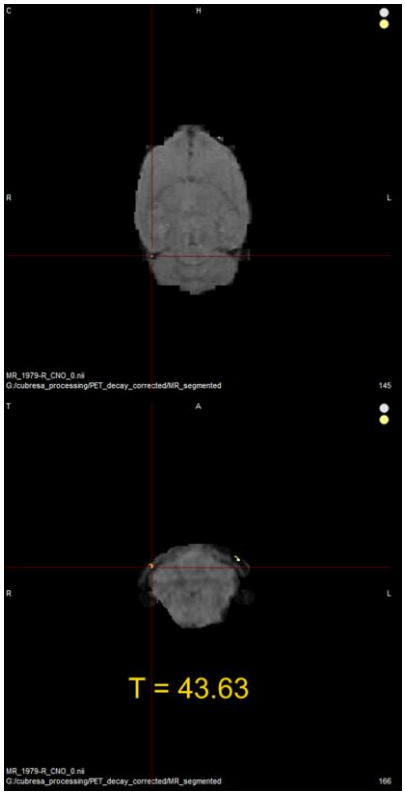

This rat showed statistically increased uptake in the outer edge of the brain (T = 43.63). This spot is suspect, however, since the size of this region of higher T value is smaller than the spatial resolution of the PET scanner and also appears near the edge of the brain volume. It is likely an artifact due to small mismatches in the size of the ROI defining the "brain" region of the saline and CNO PET images.

Rat 1981-2R

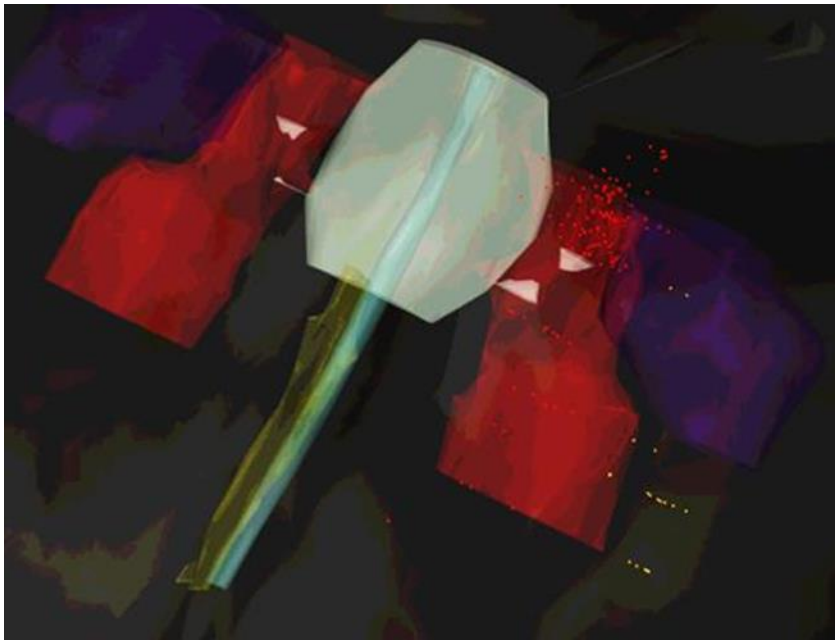

Rat 1981R had ample neurons indicating the reporter protein (m-Cherry) for the designer receptors. The mCherry+ cells were located between -13.32 and -10.08 rostro-caudally from Bregma and most mCherry+ cells are localized at the level of the rostral half of the cranial nucleus. (E. Couto done reconstruction with MBF Neurolucida, Zeiss scope, 418, purple is VII cranial nucleus, red is LPGi).

This rat showed no statistically significant differences in uptake between the two PET imaging sessions. Multiple checks to ensure that its data sets were processed correctly have found no user-induced error that could lead to this result.

Rat 1989-R

This rat also showed no statistically significant differences between the CNO and saline PET imaging sessions.

Rat 2624

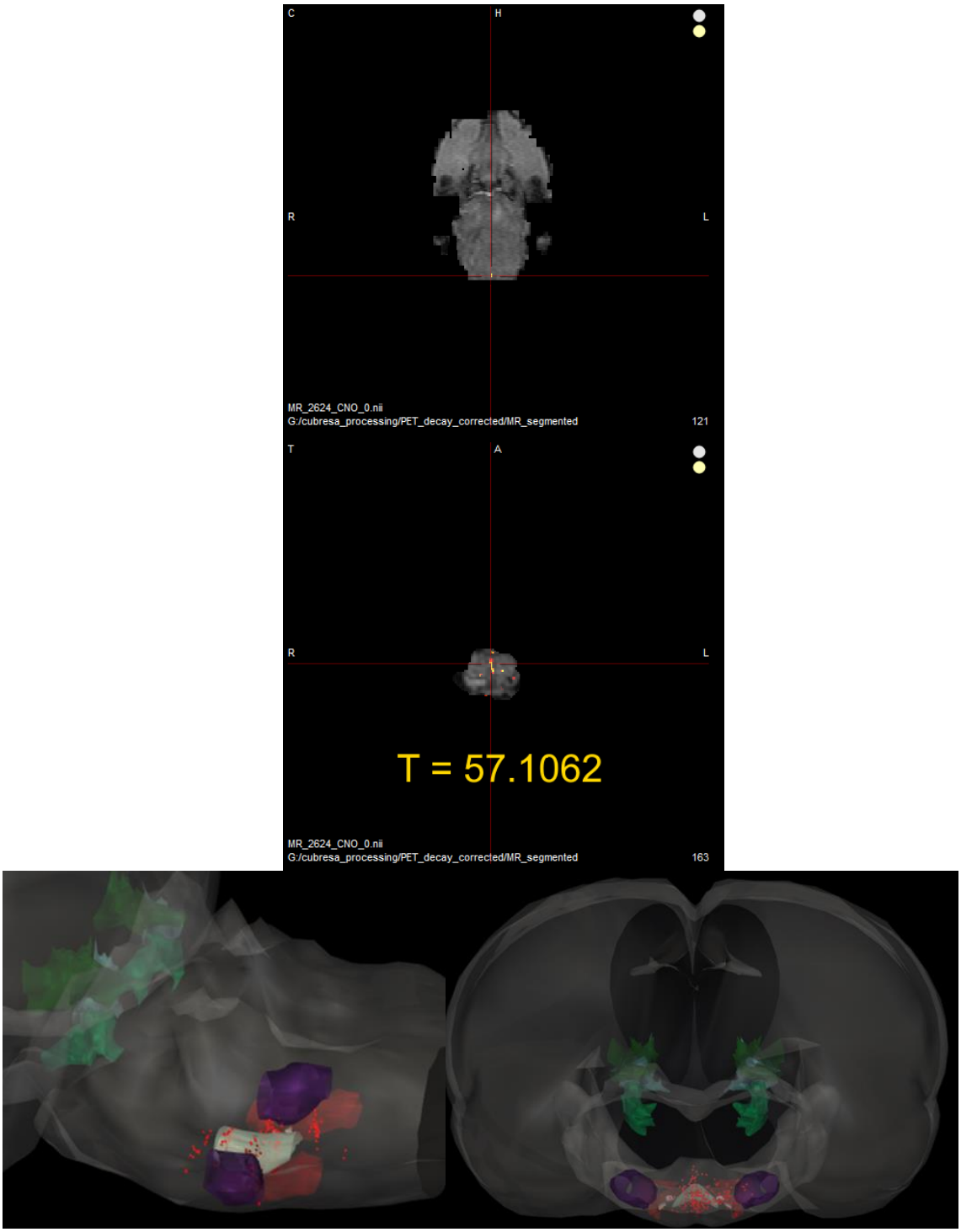

Rat 2624 showed a cluster of increased FDG uptake in the CNO imaging session near the rear of the brain. This region is large enough to potentially not be due to single-voxel ROI

mismatches, and could represent detected activation of the DREADD neurons. This cluster appears at the back of the cerebellum in lobule 9.

Rat 2624 showed m-cherry positive cells in the midline and laterally in a location that corresponds to the location of serotonergic cells. The rostro-caudal extent is approximately from -13.32 to -9.96.

Rat 2625

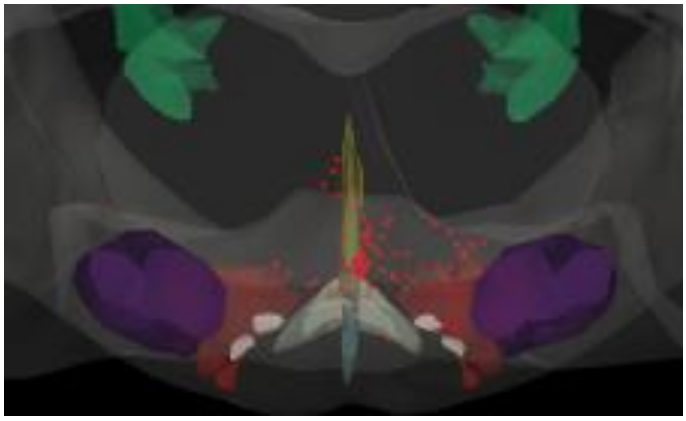

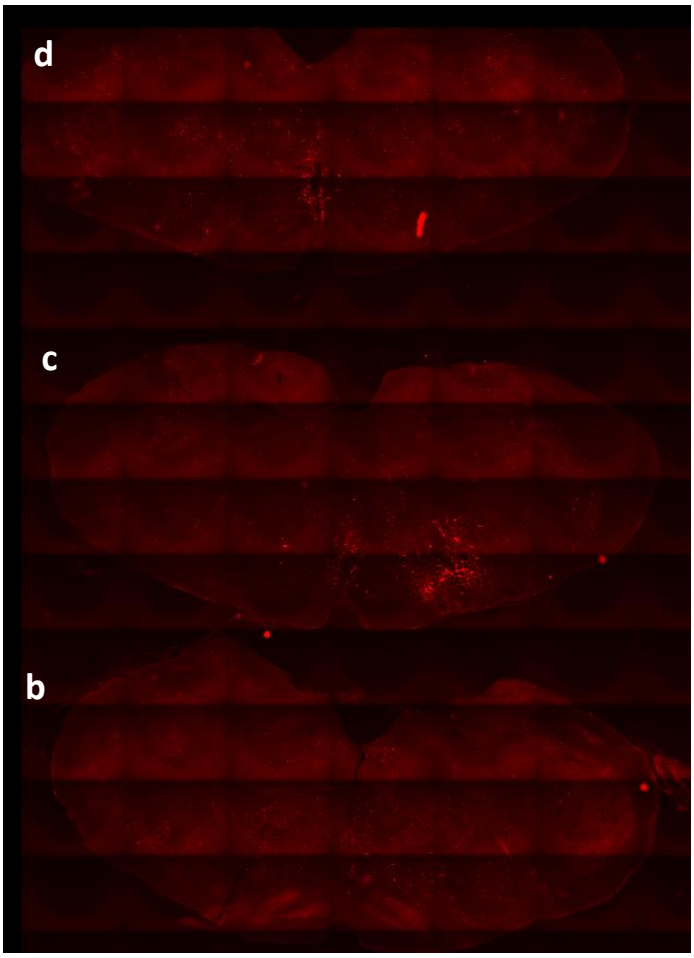

Rat 2625 showed no statistically significant differences in FDG uptake in the brain between imaging sessions treated with saline and CNO. 2625 had m-Cherry positive neurons, in the midline and laterally in a location that corresponds to the location of serotonergic cells. The rostrocaudal extent is approximately from B-13.08 to B-11.64.

Results – fMRI

For all fMRI data sets in this study, no statistically significant differences were found between imaging sessions with saline and with CNO injected. Summing axial slices to improve the SNR of the images did not change the results; combining all five slices into a single slice or combining slices 1 + 2, 2 + 3, and 3 + 4 showed no change in the SPM analysis.

Discussion

Out of the five rats in this study, only rat 2624 showed a statistically significant increase in FDG uptake when treated with CNO versus a saline injection. Assuming that the animals in question have DREADD cells properly implanted that are activated by CNO, the most obvious reason for this study's failure is that the PET data sets lack the sensitivity and/or quantitative accuracy to visualize the differences in uptake for these clusters of neurons. Increasing the radiation dose to ~37 MBq/injection could improve the signal to noise ratio of the images, but differences in brain activity should be detectable with the level of activity that was injected in this study.

Based on information provided by Katrina Armstrong, the DREADD-activated neurons should appear in the ventral medulla rather than the rat cerebellum as was seen in rat 2624. They should also appear further forward in the brain than what was seen in the imaging study.

Analysis of the fMRI data also failed to show statistically significant signal changes in the DREADD treated region of the brain. The next step for this study should be to image rats using simultaneous FDG-PET and fMRI while applying a controlled stimulus. Stimulating the rat's whiskers should increase activity in the somatosensory cortex of the rat brain, which can be easily picked up on both FDG-PET and fMRI imaging based on prior studies (Michaelides et al, J. Clin. Invest. 2013;123(12):5342-5350, doi 10.1172/JCI72117). This will allow us to determine whether our inability to image DREADD activation is due to the problems with the imaging protocols, insufficient quality of the images, or issues with the DREADD neurons not activating properly in the rat brains.

One way to improve image quality would be to increase the injected activity to nominally 37 MBq for each animal. This is a standard dose for rat neuroimaging and was used in the Michaelides study referenced above, and would provide a greater chance of detecting small differences in uptake between CNO and saline-injected animals.

Additionally, we need to determine whether the image reconstruction parameters we are using for OSMALPOSL image reconstruction are appropriate for the number of coincidence events in these fifteen minute images. A study of quantitative accuracy and spatial resolution on an image quality phantom is necessary to obtain this information.

Appendix: Normalized Voxel Value Plots

To investigate whether there was any difference in the PET data being given to the SPM analysis, a region of interest (ROI) covering the medulla of the rat was drawn on each animal. The mean voxel value of the ROI was recorded at each time point, and the standard deviation of the ROI was used to draw error bars.

Across all rats imaged in this study there was no increased uptake of FDG in CNO-treated animals compared to saline animals beyond one standard deviation.

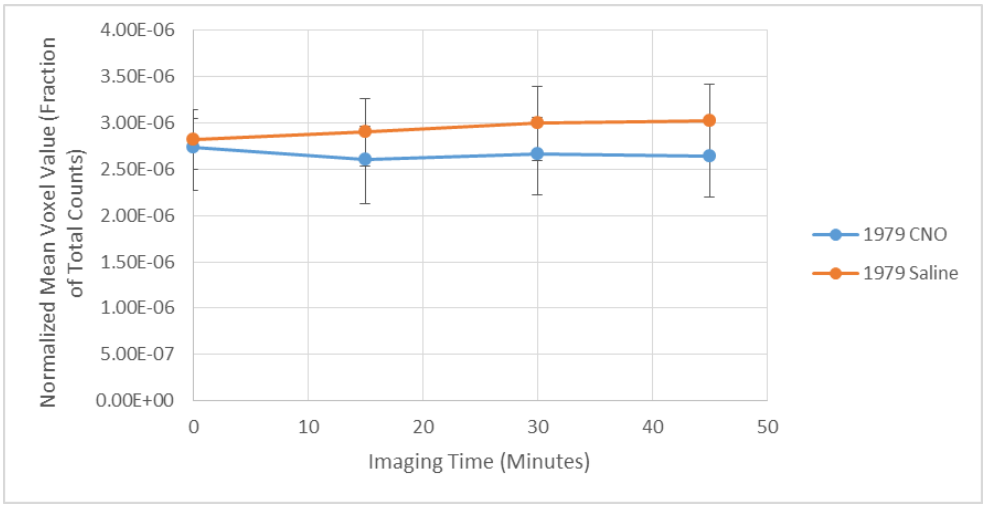
Normalized Mean Voxel Value (Fraction of Total Counts)
4.00E-06
3.50E-06
3.00E-06
2.50E-06
2.00E-06
1.50E-06
1.00E-06
5.00E-07
0.00E+00
0
10
20
30
40
50
Imaging Time (Minutes)
1979 CNO
1979 Saline

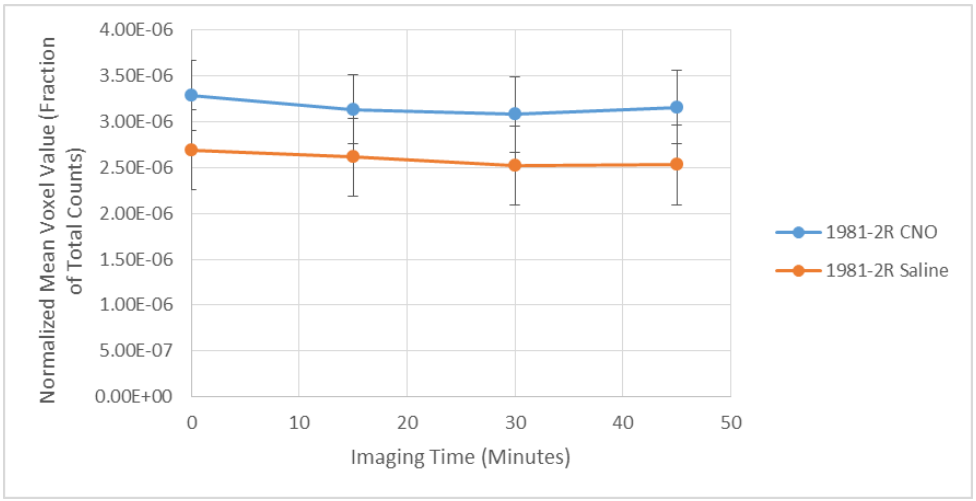
Normalized Mean Voxel Value (Fraction of Total Counts)
4.00E-06
3.50E-06
3.00E-06
2.50E-06
2.00E-06
1.50E-06
1.00E-06
5.00E-07
0.00E+00
0
10
20
30
40
50
Imaging Time (Minutes)
1981-2R CNO
1981-2R Saline

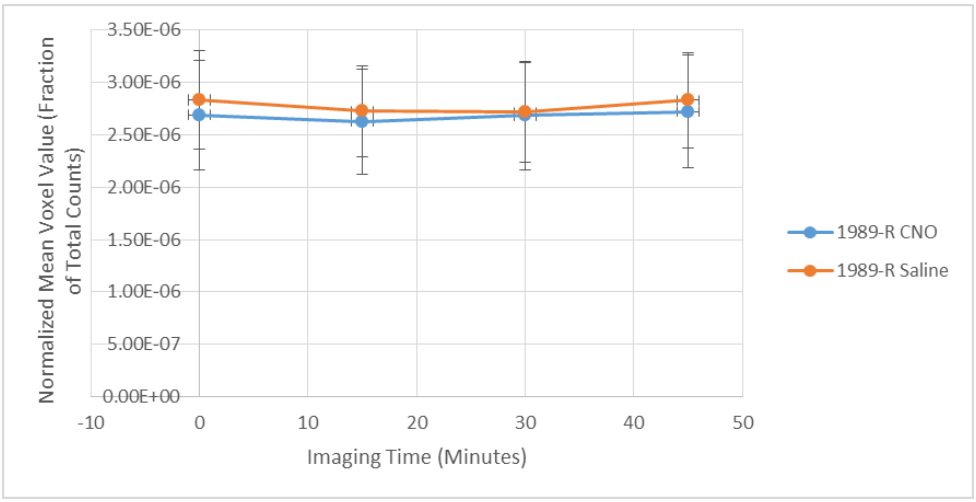
Normalized Mean Voxel Value (Fraction of Total Counts)
3.50E-06
3.00E-06
2.50E-06
2.00E-06
1.50E-06
1.00E-06
5.00E-07
0.00E+00
-10
0
10
20
30
40
50
Imaging Time (Minutes)
1989-R CNO
1989-R Saline

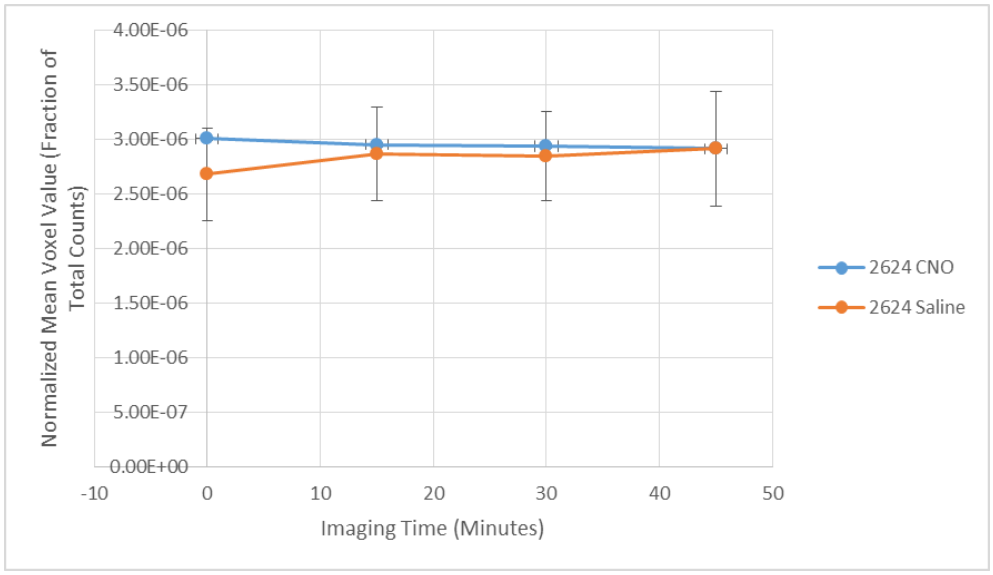
Normalized Mean Voxel Value (Fraction of Total Counts)
4.00E-06
3.50E-06
3.00E-06
2.50E-06
2.00E-06
1.50E-06
1.00E-06
5.00E-07
0.00E+00
-10
0
10
20
30
40
50
Imaging Time (Minutes)
2624 CNO
2624 Saline

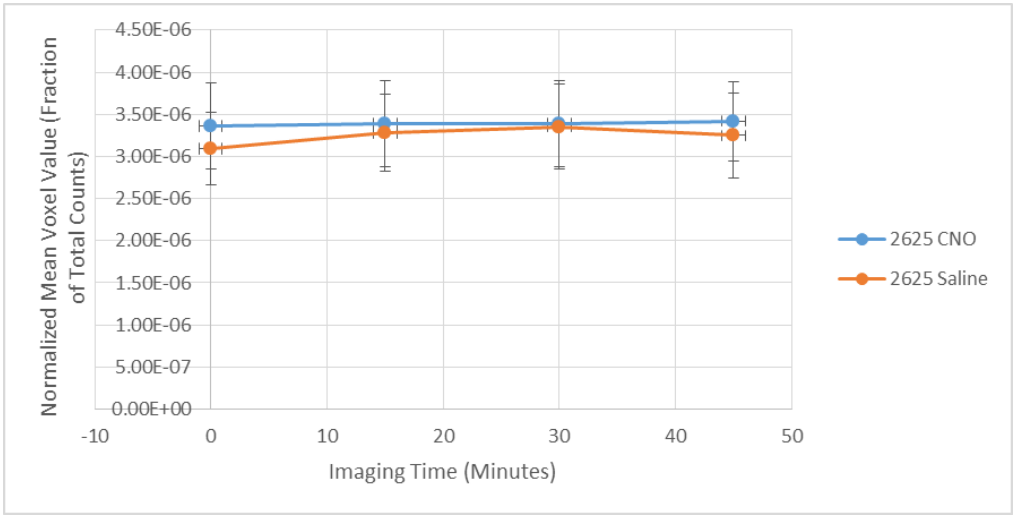
Normalized Mean Voxel Value (Fraction of Total Counts)
4.50E-06
4.00E-06
3.50E-06
3.00E-06
2.50E-06
2.00E-06
1.50E-06
1.00E-06
5.00E-07
0.00E+00
-10
0
10
20
30
40
50
Imaging Time (Minutes)
2625 CNO
2625 Saline